

**Decoding long-term trends in the wet deposition of sulfate, nitrate
and ammonium after reducing the perturbation from climate
anomalies**

Xiaohong Yao¹, Leiming Zhang²

¹Key Lab of Marine Environmental Science and Ecology, Ocean University of China,
Qingdao 266100, China

²Air Quality Research Division, Science and Technology Branch, Environment and
Climate Change Canada, Toronto, Canada

Correspondence to: X. Yao (xhyao@ouc.edu.cn) and L. Zhang (leiming.zhang@canada.ca)

1 **Abstract.** Long-term trends of wet deposition of inorganic ions are affected by multiple
2 factors, among which emission changes and climate conditions are dominant ones. To
3 assess the effectiveness of emission reductions on the wet deposition of pollutants of
4 interest, contributions from these factors to the long-term trends of wet deposition must
5 be isolated. For this purpose, a two-step approach for preprocessing wet deposition data
6 is presented herein. This new approach aims to reduce the impact of climate anomalies
7 on the trend analysis so that the impact of emission reductions on the wet deposition
8 can be revealed. This approach is applied to a two-decade wet deposition dataset of
9 sulfate (SO_4^{2-}), nitrate (NO_3^-) and ammonium (NH_4^+) at rural Canadian sites. Analysis
10 results show that the approach allows for statistically identifying inflection points on
11 decreasing trends in the wet deposition fluxes of SO_4^{2-} and NO_3^- in northern Ontario
12 and Québec. The inflection points match well with the three-phase mitigation of SO_2
13 emissions and two-phase mitigation of NO_x emissions in Ontario. Improved
14 correlations between the wet deposition of ions and their precursors' emissions were
15 obtained after reducing the impact from climate anomalies. Furthermore, decadal
16 climate anomalies were identified as dominating the decreasing trends in the wet
17 deposition fluxes of SO_4^{2-} and NO_3^- at a western coastal site. Long-term variations in
18 NH_4^+ wet deposition showed no clear trends due to the compensating effects between
19 NH_3 emissions, climate anomalies, and chemistry associated with the emission changes
20 of sulfur and nitrogen.

21

22 **1. Introduction**

23 To assess the long-term impacts of acidifying pollutants on the environment, the wet
24 deposition of sulfate (SO_4^{2-}), nitrate (NO_3^-) and ammonium (NH_4^+), among other
25 inorganic ions, has been measured for several decades through monitoring networks

26 such as the European Monitoring and Evaluation Programme (EMEP) (Fowler et al.,
27 2005, 2007; Rogora et al., 2004, 2016), the National Atmospheric Deposition
28 Program/National Trends Network in the U.S. (Baumgardner et al., 2002; Lehmann et
29 al., 2007; Sickles & Shadwick, 2015), and the Canadian Air and Precipitation
30 Monitoring Network (CAPMoN) (Vet et al., 2014; Zbieranowski and Aherne, 2011).
31 The high-quality data collected from these networks have been widely used to quantify
32 the atmospheric deposition of acidifying pollutants (Lajtha & Jones, 2013; Lynch et al.,
33 2000; Pihl Karlsson et al., 2011; Strock et al., 2014; Vet et al., 2014). The data have
34 also been utilized to identify trends in the atmospheric deposition of reactive nitrogen
35 (Fagerli & Aas, 2008; Fowler et al., 2007; Lehmann et al., 2007; Zbieranowski and
36 Aherne, 2011) and to examine the impacts of acid rain and the perturbation of the
37 natural nitrogen cycle on sensitive ecosystems (Wright et al., 2018). The long-term data
38 can also be used for assessing the effectiveness of environmental policies (Butler et al.,
39 2005; Li et al., 2016; Lloret & Valiela, 2016).

40

41 The wet deposition of SO_4^{2-} , NO_3^- and NH_4^+ is affected by not only their gaseous
42 precursors' emissions (Butler et al., 2005; Fowler et al., 2007; Li et al., 2016) but also
43 complex atmospheric processes such as long-range transport, chemical transformation,
44 and dry and wet removal (Cheng & Zhang, 2017; Yao & Zhang, 2012; Zhang et al.,
45 2012). These processes can be largely affected by climate anomalies. For example,
46 climate anomalies can sometimes bring extreme precipitation amounts in a particular
47 month and subsequently lead to extremely high wet deposition fluxes of ions through
48 enhanced wet removal of air pollutants.. Furthermore, climate anomalies can alter the
49 relative contributions of local sources versus long-range transport to the total wet
50 deposition amounts at reception sites, thereby complicating the relationships between

51 wet deposition and the emission of air pollutants of interest (Lloret & Valiela, 2016;
52 Monteith et al., 2016; Pleijel et al., 2016; Wetherbee & Mast, 2016). The emissions of
53 SO₂ and NO_x have been decreasing substantially in Europe and North America (Butler
54 et al., 2005; Li et al., 2016; Pihl Karlsson et al., 2011); coincidentally, climate anomalies
55 have also occurred more frequently in the recent decades (Burakowski et al., 2008;
56 Lloret & Valiela, 2016; Wijngaard et al., 2003), thereby leading to more complicated
57 linkages between wet deposition and emission trends on decadal scales.

58

59 Many trend analysis studies in the literature simply examined annual or seasonal values
60 as the data inputs for two popular trend analysis tools, i.e., the Mann-Kendall (M-K)
61 and linear regression (LR) methods (Marchetto et al., 2013; Waldner et al., 2014 and
62 references therein). These studies focused on the detection of statistically significant
63 trends; for example, Waldner et al. (2014) conducted a comprehensive analysis on the
64 applicability of the techniques to different choices of length and temporal resolutions
65 of a data series. Regarding the resolved trend results, these approaches are not well
66 suited to separating the impact of air pollutants' mitigation from the perturbation by
67 climate anomalies. Large uncertainties thus existed in the studies interpreting the major
68 driving forces determining the extracted trends in the wet deposition of SO₄²⁻, NO₃⁻ and
69 NH₄⁺. Regarding that air pollutant's emission mitigation targets often vary in different
70 phases of the entire study period, inflection points may exist in the trends in the wet
71 deposition of ions. The inflection points were rarely studied, despite their importance
72 for assessing the effectiveness of environmental policies. An alternative would be to
73 use high time resolution data in the Ensemble Empirical Mode Decomposition (EEMD)
74 method (Wu & Huang, 2009); however, this method still suffers from the end effect in
75 certain scenarios, whereby the extracted trends cannot be explained (Yao & Zhang,

76 2016).

77

78 A new approach is presented herein that aims to reduce the perturbations from climate
79 anomalies on data inputs so that robust trends can be elucidated for evaluating the
80 effectiveness of emission control policies. In this approach, raw data are preprocessed
81 to generate a new variable, which is then applied to M-K and LR methods. A piecewise
82 linear regression (PLR) is also used to extract trends for cases in presence of inflection
83 points. The extracted trends in the wet deposition data on a decadal scale are then
84 properly linked to major driving forces such as emission reductions and climate
85 anomalies. This new approach is first applied to the wet deposition data of SO_4^{2-} , NO_3^-
86 and NH_4^+ in Canada, as an example to demonstrate its capability and advantages over
87 the traditional approaches. The extracted trends in the wet deposition of ions are further
88 studied through correlation analysis with known emission trends of their respective
89 gaseous precursors (SO_2 , NO_x and NH_3) in Canada and the U.S. Major driving forces
90 for the trends of ion wet deposition and how the wet deposition ions responded to their
91 precursors' emissions in Canada are then revealed.

92

93 **2. Methodology**

94 *2.1 Data sources*

95 Wet deposition flux (F_{wet}) data were obtained from CAPMoN
96 ([https://www.canada.ca/en/environment-climate-change/services/air-](https://www.canada.ca/en/environment-climate-change/services/air-pollution/monitoring-networks-data/canadian-air-precipitation.html)
97 [pollution/monitoring-networks-data/canadian-air-precipitation.html](https://www.canada.ca/en/environment-climate-change/services/air-pollution/monitoring-networks-data/canadian-air-precipitation.html)). Data from four
98 sites have been collected for over twenty years and were chosen herein to illustrate the
99 novel trend analysis method (Table S1). Site 1 is an inland forest site at Chapais in
100 Québec. Site 2 is situated in a coastal forest area at Saturna in British Columbia. Sites

101 3 and 4 are two inland forest sites at the Chalk River and at Algoma, respectively, in
102 northern Ontario. Details on data sampling, chemical analysis and quality control can
103 be found in previous studies (Cheng & Zhang, 2017; Vet & Ro, 2008; Vet et al., 2014).
104 The emissions data of gaseous precursors were downloaded from the Air Pollutant
105 Emission Inventory (APEI, <https://pollution-waste.canada.ca/air-emission-inventory/>)
106 in Canada and from the USEPA National Emissions Inventory (NEI,
107 <https://www.epa.gov/air-emissions-inventories/air-emissions-sources>) in the U.S.
108 These data were demarcated at a provincial level in Canada and at a state level in the
109 U.S. Data for the years of 1990 to 2011, which correspond to the period of selected F_{wet}
110 data, were used in this study.

111

112 *2.2 Statistical methods*

113 The M-K method is a popular nonparametric statistical procedure that can yield
114 qualitative trend results, such as “an increasing/decreasing trend with a P value of
115 <0.05 ,” “a probable increasing/decreasing trend with a P value of $0.05-0.1$,” “a stable
116 trend with a P value of >0.1 , as well as a ratio of <1.0 between the standard deviation
117 and the mean of the dataset,” and “a no trend for $P>0.1$ with all other conditions”
118 (Kampata et al., 2008; Marchetto et al., 2013). The LR method has also been widely
119 used to extract trends (Marchetto et al., 2013; Waldner et al., 2014). Zbieranowski and
120 Aherne (2011) used LR to extract trends by separating different phases because of the
121 presence of inflection points in the entire study period, and the approach is same as PLR
122 (Vieth, 1989). In this study, the three methods were employed to compute the trends
123 of ion wet deposition using software downloaded from [https://www.gsi-](https://www.gsi-net.com/en/software/free-software/gsi-mann-kendall-toolkit.html)
124 [net.com/en/software/free-software/gsi-mann-kendall-toolkit.html](https://www.gsi-net.com/en/software/free-software/gsi-mann-kendall-toolkit.html) and Excel 2016, first
125 using the annual F_{wet} directly as input data, then using a modified input data set, as

126 described in Section 2.3.

127

128 The annual F_{wet} is widely used for trend analysis and the trend results are thereby used
129 to compare with those derived from the approach proposed in this study. Note that R^2
130 is conventionally used in LR and PRL. However, r instead of R^2 is used in correlation
131 analysis. Thus, R^2 and r are used for the two types of analyses in this study, respectively
132 Moreover, several methods can be used to do PRL in classical statistics literature. The
133 simplest one is to manually conduct piecewise regression where inflection points are
134 visible to be recognized, and this approach is used in this study. More complex
135 algorithms are also available in literature to conduct PRL for datasets with hundreds of
136 points (Ryan and Porth, 2007 and references therein). The complex algorithms have
137 seldom been used to identify trends in annual wet deposition of ions because of the
138 short data record.

139

140 *2.3 Filtering climate anomalies*

141 The modified input data set was produced in two steps. The first step was an effort to
142 reduce the perturbation from the monthly climate anomalies to the input data. This was
143 done by creating a new variable that was defined as the slopes of the regression
144 equations of a series of study years against a climatology (base) year using monthly
145 F_{wet} data. Note that the monthly F_{wet} data were aggregated from daily raw data before
146 the regression analysis. To ensure the presence of enough data points in each regression
147 equation, the data corresponding to two-year periods (or 24 monthly F_{wet} values) were
148 grouped together, as detailed below. At a selected site and for a given chemical
149 component, monthly F_{wet} data were generated for the first two years and were grouped
150 together and rearranged from the smallest to the largest values to form an array of data

151 with 24 data points, i.e., $A(i)$ with $i=1$ to 24. Repeating the above procedure for the
152 subsequent years using a two-year interval to eventually obtain a series of data arrays,
153 $A(i)$ now becomes $A(i, j)$ with $i=1$ to 24 and $j=1$ to N , where N is the total number of
154 data arrays. The climatology data array ($CA(i)$) was then defined as the average of all
155 of the arrays as follows:

$$156 \quad CA(i) = \frac{1}{N} \sum_{j=1}^N A(i, j), \quad i = 1 \text{ to } 24.$$

157

158 LR with zero interception was applied for each individual data array against the
159 climatology data array. In cases where the maximum monthly deposition flux deviated
160 greatly from the general regression curve, the slopes (m-values) were calculated after
161 excluding the maximum monthly deposition flux, which is an approach that reduced
162 the perturbation to the m-values from the monthly scale climate anomalies. The second
163 step was to screen out the outliers in m-values, which reduced the perturbation to the
164 m-values from the annual-scale climate anomalies.

165

166 *2.4 Example case for data filtering*

167 An analysis of Site 1 is used to illustrate the new approach and demonstrate its
168 advantages against the existing common approaches used in the literature. Twelve two-
169 year periods of data (1988-1989, 1990-1991, etc.) are available from this site. The
170 regression of each data set against the climatology data set was first performed using
171 all of the monthly values to obtain an m-value (the slope) (Fig. 1a-d). For eight out of
172 the 12 data sets, the m-values were recalculated after excluding the maximum monthly
173 value of F_{wet} , which appeared to be an apparent outlier of the linear regression. Three
174 out of the 12 data sets showed the maximum F_{wet} being positively deviated from the
175 general trend, five negatively deviated from the general trend, and four consistent with

176 the general trend. The R^2 values were then significantly increased for the eight sets,
177 e.g., from the original values of 0.79-0.94 to the improved values of 0.92-0.98. To
178 demonstrate that the excluded maximum value was an outlier, the case of the 1990-
179 1991 data set was taken as an example. The new regression equation ($y=1.47x$, $R^2=0.98$,
180 Fig. 1a) predicted a maximum value in the range of 330-368 $\text{mg m}^{-2} \text{month}^{-1}$ using three
181 times the standard deviation ($\pm 3 \text{ SD}$, 0.08) at a 99% confidence level. The actual
182 observed maximum value of 532 $\text{mg m}^{-2} \text{month}^{-1}$ was much larger than the upper range
183 of the predicted value and was thus believed to be caused by monthly scale climate
184 anomalies, i.e., the occurrence of extreme amount of precipitation. The maximum
185 monthly deposition flux in 1990-1991 occurred in September 1990 when the monthly
186 precipitation depth reached 294 mm, which was much higher than those in the same
187 month of other years, e.g., 169, 68, 95 and 127 mm in 1988, 1989, 1991 and 1992,
188 respectively. The maximum daily precipitation depth in September was also higher in
189 1990 (91 mm) than in other years (43.6, 12.2, 13.6 and 26.8 mm in 1988, 1989, 1991
190 and 1992, respectively). However, the monthly geometric average concentration of
191 SO_4^{2-} in precipitation (1.8 mg L^{-1}) in September 1990 was close to the mean value
192 ($1.7 \pm 0.3 \text{ mg L}^{-1}$) in September 1988-1992 and was even smaller than that (2.9 mg L^{-1})
193 in August 1990. The maximum value was treated as an outlier and excluded for
194 analysis.

195

196 Using the similar procedure, all outliers in this study were identified. The exclusion of
197 the observed maximum value greatly reduced the perturbation of the short-term climate
198 anomalies to the calculated m-value in this two-year period, i.e., the m-value decreased
199 from 1.67 to 1.47, which in turn increased the relative contribution of the air pollutants'
200 emissions to the calculated m-value. Note that monthly changes in emissions may not

201 impact the F_{wet} as much as does a large monthly change in precipitation depth or
202 concentration in precipitation. For example, the monthly average concentrations of SO_2
203 were almost the same in May, September and October of 1990 ($\sim 0.7 \mu\text{g m}^{-3}$) while the
204 monthly F_{wet} of SO_4^{2-} varied significantly, e.g., 113, 179 and $532 \text{ mg m}^{-2} \text{ month}^{-1}$,
205 respectively in the same months. The monthly average concentration of SO_2 in February
206 ($4.8 \mu\text{g m}^{-3}$) was the largest among the twelve months of 1990, but the corresponding
207 monthly F_{wet} of SO_4^{2-} was the smallest ($34 \text{ mg m}^{-2} \text{ month}^{-1}$).

208

209 Even through comprehensive analysis, any single climate factor alone, including
210 monthly precipitation depth, was apparently unable to explain the negative deviation of
211 the maximum monthly value of F_{wet} from the general trend. The causes of such a
212 negative deviation is yet to be identified. In summary, the new approach proposed
213 above by applying the criteria of being outside the boundaries of ± 3 times the standard
214 deviation of the general trend meets the objective of identifying outlier data points.

215

216 The revised m-values were further scrutinized by eliminating the outliers caused by the
217 annual-scale climate anomalies. For example, the m-value of 1.31 in 1998-1999 greatly
218 deviated from other m-values, narrowly oscillating approximately 0.96 ± 0.07 (average
219 $\pm 1 \text{ SD}$) during the period of 1994-2005, even with the $\pm 3 \text{ SD}$ being considered (Fig.
220 1a-d). Using the value of 0.96 as the reference, climate anomalies likely increased the
221 F_{wet} of SO_4^{2-} by 37% in 1998-1999. The m-values were then calculated by shifting one
222 year in time to 1997-1998 (1.07) and to 1999-2000 (1.24). The F_{wet} in 1998 was less
223 affected by climate anomalies than that in 1999. Thus, the m-value in 1997-1998 was
224 within 0.96 ± 0.21 (average $\pm 3 \text{ SD}$) and used to replace the m-value in 1998-1999 for
225 the trend analysis. Similar to the first step discussed above, this approach meets the

226 objective of identifying outlier m-values by applying the criteria of being outside the
227 range of ± 3 SD plus the average m-value during a decade or a longer period. The
228 abnormally increased F_{wet} of SO_4^{2-} in 1999 was mainly because of the increased
229 precipitation depth (1312 mm), which was the largest during 1998-2011 (the annual
230 average precipitation depth excluding 1999 was 1067 ± 86 mm). However, the geometric
231 average concentration of SO_4^{2-} in precipitation in 1999 (1.0 mg L^{-1}) was close to those
232 in the other years, e.g., 0.9 mg L^{-1} in 1997 and 1998 and 1.0 mg L^{-1} in 2000.

233

234 *2.5 Justification for the new approach* More justification of the new approach can be
235 found in the Supporting Information, including Figs. S1-6, wherein the statistical
236 comparison between this and other approaches was presented. Theoretically, the
237 extracted trend using the data preprocessed with the new approach is determined by the
238 local emissions of air pollutants, the regional transport of air pollutants, and climate
239 anomalies that are unable to be removed by the new approach. It is assumed that the
240 extracted trend is less affected by microphysical/chemical processes, since two-year
241 data were used together to calculate the m-value.

242

243 In theory, if the data from different sites in the same region are grouped together for
244 trend analysis, the results may be better linked to the trends of the regional emissions
245 of related air pollutants. In the following sections, trend analysis results from individual
246 sites as well as those from grouped sites are discussed. Sites 1, 3 and 4 showed similar
247 trends in the wet deposition of SO_4^{2-} and NO_3^- , and these three sites were grouped
248 together.

249

250 **3. Results and discussion**

251 *3.1 Trends at Site 1 after reducing perturbations from climate anomalies*

252 Trends in the m-values shown in Fig. 2 represent the trends after removing the
253 perturbations from climate anomalies at Site 1 in northern Québec from 1988 to 2011.
254 SO_4^{2-} and NO_3^- showed decreasing trends from a LR analysis, with R^2 values of 0.81
255 and 0.71, respectively, and P values <0.01 (Fig. 2a and 2d). The decreasing trends were
256 also confirmed by the M-K method analysis. NH_4^+ exhibited a stable trend from M-K
257 analysis (Fig. 2g), as well as no significant trend with P value >0.05 from LR analysis.
258 The annual F_{wet} of these ions are also shown in Figs. 2b, 2e and 2f and annual emissions
259 of SO_2 , NO_x and NH_3 in Figs. 2c, 2f and 2i, respectively. These data were used to
260 compare and facilitate analysis in terms of identifying inflection points and the
261 advantage of using the m-value over the annual F_{wet} , as presented below.

262

263 The m-values of SO_4^{2-} and NO_3^- also allowed for statistical identification of trends in
264 different phases supported by annual variations in emissions of SO_2 and NO_x (Figs. 2c
265 and 2f) to some extent. The inflection point for each phase is critical to a) link the annual
266 F_{wet} of ions and the emissions of the corresponding precursors, and b) assess the
267 effectiveness of environmental policies. For example, the trends in the m-values of
268 SO_4^{2-} can be clearly classified into three phases (Fig. 2a). Therefore, PLR should be
269 applied separately for the different phases in the presence of the inflection points, rather
270 than LR for the entire period, and the result is presented as:

$$271 \left\{ \begin{array}{l} m - \text{value} = 1.38, 1988 \leq x < 1994 \\ m - \text{value} = 1.02, 1994 \leq x \leq 2005 \\ m - \text{value} = -0.185 * \left(\frac{x}{2} - 1001\right) + 1.15, 2005 < x \leq 2010 \end{array} \right.$$

272 where x represents the calendar year from 1988 to 2010.

273 The m-values oscillated approximately 1.38 ± 0.08 during Phase 1 (1988 to 1993) and
274 approximately 1.02 ± 0.08 during Phase 2 (1994 to 2005), with a significant difference

275 between the two phases under the t-test (P value <0.01), thereby implying an abrupt
276 decrease of approximately 30% at the inflection point between the two phases. The m-
277 values linearly decreased by approximately 20% every two years, starting from the end
278 of Phase 2 to Phase 3 (2006-2011). Again, a significant difference existed between
279 Phase 2 and Phase 3 under the t-test (P value <0.01). The three phases generally aligned
280 with the three-phase regulated SO₂ emissions in Ontario. It should be stated that Phase
281 1 and Phase 3 each covered only six years (N=6). Cautions should be taken to explain
282 the trend result in each phase in relation to precursors' emissions.

283

284 The PRL result of NO₃⁻ is expressed as:

$$285 \quad \begin{cases} m - value = 1.09, 1988 \leq x < 2004 \\ m - value = -0.128 * \left(\frac{x}{2} - 1001\right) + 1.08, 2004 \leq x \leq 2010 \end{cases}$$

286 The trend in the m-values of NO₃⁻ can be classified into two phases with the inflection
287 point at 2003, which was confirmed by the t-test result, i.e., the values oscillated
288 approximately 1.09±0.09 during the period from 1988 to 2003 and then exhibited a
289 significant decrease of approximately 50% overall afterwards, with P value <0.01.

290 The m-value of NO₃⁻ in 1998-1999 was approximately 30% larger than the mean value
291 in 1988-2003 and exceeded the mean value plus 3 SD in 1998-2003, and thus was not
292 included in the trend analysis. The sharp increase in F_{wet} of NO₃⁻ occurred mainly in
293 1999, which was probably due to largely increased annual precipitation depth as
294 mentioned in Section 2.4. The analysis was also supported by the geometric average
295 concentration of NO₃⁻ in precipitation, which was 1.1 mg L⁻¹ in 1999, 5% lower than
296 that in 1988 and only 5-10% higher than those in 1990-1991, 1993 and 2002.
297 Moreover, the monthly F_{wet} values of NO₃⁻ in March, April, July and August 1999 were
298 actually lower than the corresponding long-term averages in 1988-2003 (excluding

299 1999) (Fig. S6a). This outcome indicates that the large increase in annual F_{wet} of NO_3^-
300 in 1999 was unlikely to have been determined by the emissions of its gaseous
301 precursors. The same can be said for the large increase in F_{wet} of SO_4^{2-} in 1999 (Fig. 2a,
302 S6b).

303

304 To demonstrate the advantage of using the m-values in trend analysis, m-values were
305 correlated to the reported emissions of concerned air pollutants. The trends in the m-
306 value of SO_4^{2-} at Site 1 (Fig. 2a) were clearly different from those of the SO_2 emissions
307 in Québec (Fig. 2c) but matched well to those in Ontario (Fig. 2c), which is also
308 supported by their Pearson correlation coefficients, e.g., no significant correlation ($r =$
309 0.46 and P value >0.05) for the former case and a good correlation ($r = 0.96$ and P value
310 <0.01) for the latter case. Zhang et al. (2008) reported that this remote area can receive
311 the long-range transport of air pollutants from Ontario but that transport is less likely
312 from the intensive emission sources in Québec.

313

314 In addition, LR analysis of the annual F_{wet} of SO_4^{2-} revealed a decreasing trend (second
315 row in Fig. 2b). The M-K method analysis also confirmed the decreasing trend with
316 annual F_{wet} as input. However, the three-phase trend in F_{wet} of SO_4^{2-} and related
317 inflection points, identified using the m-values discussed above, were not identified by
318 the t-test when simply using annual F_{wet} data as input. Identifying these inflection points
319 is crucial to assess the effectiveness of environmental policies. The correlation between
320 annual F_{wet} and emission was 0.89 for SO_4^{2-} vs. SO_2 in Ontario (P values <0.01), while
321 the corresponding r value was as high as 0.96 between m-value and emission. After
322 reducing the perturbations from climatic factors to the annual F_{wet} , a stronger
323 correlation was obtained between F_{wet} and emission. The increased r further solidified

324 the dominant contribution of the long-range transport of air pollutants from Ontario
325 rather than Québec to the wet deposition of SO_4^{2-} at Site 1.

326

327 The trends in NO_x emissions during 1990-2003 had similar bell-shape patterns in
328 Québec and Ontario, although with different magnitudes of emissions (Fig. 2f). A
329 different trend pattern was seen for the m-value of NO_3^- at Site 1 than for the
330 abovementioned provincial emissions during the same period (Fig. 2d), and there was
331 no significant correlation ($r < 0.41$, with P value > 0.05) between the m-value of NO_3^-
332 and the emissions of NO_x in Québec or Ontario. Different results were found for the
333 period of 2002-2011 than those of 1990-2003 discussed above. In 2002-2011, the m-
334 value of NO_3^- decreased by ~50% and the NO_x emissions decreased by ~40% in
335 Québec and Ontario; also, good correlations ($r = 0.94-0.95$ with P values < 0.01) were
336 observed between m-values and emissions. The contrasting correlation results between
337 the two different periods discussed above implied the complex link between wet
338 deposition of NO_3^- and emissions of NO_x . One might assume that the perturbation from
339 climate anomalies might not be fully removed by the new approach for the period of
340 1990-2003, which overwhelmed the effects of NO_x emissions on the trends in m-values
341 of NO_3^- . Such a possibility is practically very low since the approach works well for the
342 period of 2002-2011. The contrasting results between these two periods are yet to be
343 explained. F_{wet} of NO_3^- and precipitation depth exhibited only a weakly significant
344 correlation, with $r = 0.58$ and $P < 0.05$ in 1988-2003 (the values in 1999 were excluded).
345 Annual precipitation varied by only ~20% during the fifteen years, and this factor alone
346 was unlikely to explain the ~100% interannual variation of F_{wet} of NO_3^- during that
347 period.

348

349 LR analysis of the annual F_{wet} of NO_3^- revealed a decreasing trend (second row in Fig.
350 2e), confirmed by the M-K method analysis. However, the two-phase trend in F_{wet} of
351 NO_3^- and related inflection point were not identified by the t-test when simply using
352 annual F_{wet} data as input. The correlations between annual F_{wet} and emission were 0.74-
353 0.76 for NO_3^- vs. NO_x in Québec and Ontario (P values <0.01), while the corresponding
354 r values increased to 0.84-0.85 between m-value and emission. Both the identified
355 inflection point and the stronger correlation between m-value and emission
356 demonstrated the advantage of using the m-value over annual F_{wet} of NO_3^- in trend
357 analysis.

358

359 The m-value of NH_4^+ at Site 1 had no significant correlation ($r = 0.21$ and P value >0.05)
360 with the emission of NH_3 in Québec but exhibited a weakly significant correlation ($r =$
361 0.60 and P value <0.05) with the emission of NH_3 in Ontario. Nearly all of the NH_4^+
362 was associated with SO_4^{2-} and NO_3^- in the atmosphere (Cheng and Zhang, 2017; Teng
363 et al., 2017; Tost et al., 2007; Zhang et al., 2012), and the trends in the m-value of NH_4^+
364 could be affected by many other factors besides NH_3 emissions and climate anomalies,
365 e.g., gas-aerosol partitioning and different dry and wet removal efficiencies between
366 NH_3 and NH_4^+ , pH value of wet deposition.

367

368

369 The stable trend in annual F_{wet} of NH_4^+ and the decreasing trend in annual F_{wet} of NO_3^-
370 gradually increased the relative contributions of reduced nitrogen in the total nitrogen
371 wet deposition budget, e.g., from 40% in 1998-1999 to 52% in 2010-2011. A similar
372 trend has also been recently reported in the U.S. (Li et al., 2016). Such a trend was
373 mostly due to the mitigation of NO_x rather than climate anomalies.

374

375 *3.2 Decadal climate anomalies drove trends at Site 2*

376 *3.2.1 Trends in m-value of SO₄²⁻*

377 Fig. 3 shows the trend analysis results at Site 2. An obvious shift in the m-values and
378 annual F_{wet} occurred during 2001-2002, as detected by the t-test, i.e., the m-values of
379 SO₄²⁻ oscillated approximately 1.15±0.11 in 1990-2001 and 0.76±0.02 in 2002-2011
380 (or 0.83±0.12 if the value in 2006-2007 was included), but with a significant difference
381 between the two periods with P value <0.01. The annual F_{wet} of SO₄²⁻ oscillated
382 approximately 632±63 mg m⁻² in 1990-2001 and 452±74 mg m⁻² in 2002-2011, and the
383 values between the two periods showed significant differences. The shift led to the m-
384 values and annual F_{wet} of SO₄²⁻ exhibiting a consistent decreasing trend by ~40% overall
385 from 1990 to 2011 using the LR and the M-K method.

386

387 The emissions of SO₂ oscillated approximately 1.13±0.07 in 1990-2001 and 1.06±0.03
388 in 2002-2011 in British Columbia, which did not support the large decrease of
389 approximately 40% in wet deposition of SO₄²⁻ in 2002-2011. Statistically, no
390 correlation existed between annual F_{wet} of SO₄²⁻ and the emissions of SO₂ in British
391 Columbia, with r = 0.52 and P value >0.05. Although the transboundary transport of air
392 pollutants from the U.S. cannot be excluded, the almost constant m-values from 2002
393 to 2011 (excluding 2006-2007) at Site 2 were inconsistent with the approximately 70%
394 decrease in emissions of SO₂ in the state of Washington in the U.S. during that period
395 (not shown). Precipitation cannot explain the jump in wet deposition either, because
396 there was no corresponding jump in precipitation during 2001-2002 (Fig. 3b).

397

398 van Donkelaar et al. (2008) analyzed aircraft and satellite measurements from the

399 Intercontinental Chemical Transport Experiment and proposed the long-range transport
400 of sulfur from East Asia to the west coast of Canada. The wind vector and wind speed
401 from the North American Regional Reanalysis (NARR), with a spatial resolution of 32
402 km by 32 km (Mesinger et al., 2006), were thereby analyzed to study the decadal
403 changes in wind fields and associated potential impacts on the long-range transport of
404 air pollutants over the western coastal Canada and U.S. The average wind fields
405 including mean wind vector and speed (shading in Fig 4a-d) in 1990-2011 at 925 hPa
406 showed air masses over the western coastal Canada and U.S. were primarily originated
407 from the Pacific Ocean (Fig. 4a). However, the anomalies of wind fields in 1990-2001
408 relative to 1990-2009 clearly showed a counterclockwise pattern in the corresponding
409 coastal area, including Site 2., while a clockwise pattern existed in 2002-2011 relative
410 to 1990-2009 (Fig. 4b, c). The anomalies shown in Fig. 4c indicated the northwesterly
411 wind being enhanced in 2002-2011 over the western coastal Canada and U.S., possibly
412 reducing air pollutants being transported from the continent to Site 2. In contrast, the
413 anomalies in Fig. 4b indicated that the northwesterly wind was reduced in 1990-2001.
414 Consequently, more air pollutants might have been transported from the continent to
415 Site 2, resulting in a distinct demarcation in 2002. This hypothesis was also supported
416 by a large rebound of the m-value in 2006-2007, due to the increase in F_{wet} of SO_4^{2-} in
417 2007. The climate anomalies of wind fields in 2007 relative to 1990-2009 showed a
418 counterclockwise pattern in the north, while the clockwise pattern was pushed to the
419 south (Fig. 4d). With the northwesterly wind being reduced, a greater contribution of
420 air pollutants from the coast of Canada and U.S. to Site 2 might have led to the large
421 increase in F_{wet} of SO_4^{2-} during a few month-long periods in 2007.

422

423 The present study is the first one identifying the decreasing trend in the annual F_{wet} of

424 SO_4^{2-} as being very likely caused by decadal climate anomalies, i.e., wind fields, rather
425 than by the emission reductions of SO_2 . The decadal anomalies of wind fields may
426 substantially alter the long-range transport of air pollutants to the reception site. Note
427 that the causes for the decadal anomalies of wind fields in this region are beyond the
428 scope of the present study, but some information can be found in the literature (Bond
429 et al., 2003; Coopersmith et al., 2014; Deng et al., 2014).

430

431 3.2.2 Trends in m-values of NO_3^- and NH_4^+

432 For the wet deposition of NO_3^- , the m-values also showed a clear shift, i.e., the m-values
433 oscillated approximately 1.09 ± 0.14 in 1990-2001 and 0.88 ± 0.06 in 2002-2011, with a
434 significant difference between the two periods under the t-test with P value < 0.01 . The
435 annual F_{wet} of NO_3^- varied substantially, and the shift could not be identified
436 statistically. However, the annual F_{wet} of NO_3^- exhibited a decreasing trend by M-K
437 method analysis. Similar to the case of SO_4^{2-} , no significant correlation ($r = 0.49$, P
438 value > 0.05) existed between the annual F_{wet} of NO_3^- and the emissions of NO_x in
439 British Columbia.

440

441 In addition to decadal anomalies of wind fields, the interannual climate variability such
442 as precipitation depth, annual anomalies of wind fields in 2007, etc., (Fig. 3b) also
443 affected the trends in m-values and annual F_{wet} of NO_3^- . The annual precipitation depth
444 largely varied from 601 mm to 1054 mm in the two decades. The perturbations from
445 interannual variability of precipitation depth cannot be completely removed by the new
446 approach. For example, the calculated m-values in 1992-1993 and 1994-1995 were
447 evidently lower than the m-values in 1990-2001. However, the annual geometric
448 average concentrations of NO_3^- in 1992-1995 varied around $0.77 \pm 0.11 \text{ mg L}^{-1}$ and were

449 even larger than the values of $0.66 \pm 0.08 \text{ mg L}^{-1}$ in 1990-2001 (excluding 1992-1995).
450 The lower m-values were mainly attributed to the lower precipitation depth in 1992-
451 1994 (Fig 3b) rather than lower emissions of NO_x. Interannual climate variability
452 including precipitation depth and annual anomalies of wind fields may complicate the
453 relationship between the F_{wet} of NO₃⁻ and the emissions of NO_x in British Columbia.
454 For example, the m-values in 1990-1991, 1996-1997, 1998-1999 and 2000-2001 were
455 nearly constant at 1.17 ± 0.03 ; however, the NO_x emissions in British Columbia in 1998-
456 1999 were 26% greater than those in 1990-1991. Moreover, there was a sharp decrease
457 in the NO_x emissions (by ~30%) from 2002 to 2011 in British Columbia. However, the
458 m-values oscillated approximately 0.88 ± 0.06 and showed no clear trend based on either
459 the M-K method or LR analysis. The interannual climate variability apparently negated
460 the impact of reduced emissions during these periods.

461

462 The m-values and the annual F_{wet} of NH₄⁺ oscillated approximately 0.99 ± 0.13 and
463 $81 \pm 16 \text{ mg m}^{-3}$, respectively, in the period of 1990-2011, and showed no trend (Fig. 3).
464 Neither the m-values nor annual F_{wet} of NH₄⁺ showed the two-period distribution
465 pattern or had any significant correlation with the emissions of NH₃ in British Columbia
466 at a 95% confidence level. Similarly to Site 1, the annual variation in F_{wet} of NH₄⁺ at
467 Site 2 cannot be simply explained by known emission trends.

468

469 In summary, decadal anomalies of wind fields overwhelmingly determined the long-
470 term trends in the wet deposition of SO₄²⁻ and NO₃⁻, with the perturbation from monthly
471 and annual climate anomalies removed at Site 2. The interannual climate variability
472 including precipitation depth, annual anomalies of wind fields, etc., further complicated
473 the trends, resulting in undetectable influences of the emission trends on the deposition

474 trends. Since the decrease in F_{wet} of NO_3^- appeared to be primarily caused by decadal
475 climate anomalies of wind fields, the relative contributions of NH_4^+ and NO_3^- in the
476 total N wet deposition varied little, i.e., 33% versus 67% in 2010-2011 and 31% versus
477 69% in 1990-1991.

478

479 *3.3 Regional trends in wet deposition in northern Ontario and Québec*

480 Trends in the m-values or annual F_{wet} of ions at Sites 3 and 4 in the northern regions of
481 Ontario were generally similar to those found at Site 1 (Figs. S7 and S8). The three-
482 phase trend in m-values of SO_4^{2-} and the two-phase trend in m-values of NO_3^- were also
483 obtained at Sites 3 and 4 after excluding a few m-values that were caused by large
484 perturbations from climate anomalies. For example, the annual precipitation depths of
485 1044 mm in 1987 and 905 mm in 1997 at Site 4 were evidently lower than the average
486 value of 1299 ± 124 mm (excluding 1987 and 1997) in 1985-1997 (Table S2). However,
487 the geometric average concentration of SO_4^{2-} of 1.5 mg L^{-1} in 1997 was the same as the
488 mean value of $1.5 \pm 0.2 \text{ mg L}^{-1}$ in 1995-1999 (excluding 1997). The value of 1.6 mg L^{-1}
489 in 1987 was also same as that in 1989. The lower annual precipitation depths in 1987
490 and 1997 than in the other years were very likely the dominant factor causing the
491 abnormally lower m-values in 1986-1987 and 1996-1997. Thus, Sites 1, 3 and 4 were
492 combined together to study regional trends in the northern areas of Ontario and Québec
493 (Fig. 5a-c). Similar to those found at the individual sites, the temporal profile of regional
494 m-values of SO_4^{2-} can be clearly classified into three phases (Fig. 5a) as follows: Phase
495 1 from 1988 to 1993 with m-values oscillating approximately 1.31 ± 0.08 , Phase 2 from
496 1994 to 2003 with near-constant m-values of 1.05 ± 0.04 , and Phase 3 for 2004 onward
497 with a decreasing trend by an overall $\sim 50\%$. Significant differences of m-values existed
498 between any two of the three phases, based on the t-test results (P value < 0.01). The

499 PRL result is expressed as below:

$$500 \quad \left\{ \begin{array}{l} m - value = 1.31, 1988 \leq x < 1994 \\ m - value = 1.05, 1994 \leq x < 2004 \\ m - value = -0.129 * \left(\frac{x}{2} - 1001 \right) + 1.03, 2004 \leq x \leq 2010 \end{array} \right.$$

501 The three-phase pattern of m-values matched well with the three-phase emission profile
502 of SO₂ in Ontario. Statistically, a ~70% decrease in m-value and a ~70% decrease in
503 emissions were found from 1990 to 2011, with a correlation of r = 0.95 (P value <0.01).

504

505 The profile of the regional m-values of NO₃⁻ also clearly exhibited two phases,
506 according to the following t-test results: Phase 1 from 1988 to 2003, with m-values
507 narrowly varying approximately 1.11±0.05, and Phase 2 from 2004 to 2011 with a
508 decreasing trend by an overall ~40% against that in 2002-2003 (Fig. 5b). The PRL
509 result is expressed as below:

$$510 \quad \left\{ \begin{array}{l} m - value = 1.11, 1988 \leq x < 2004 \\ m - value = -0.11 * \left(\frac{x}{2} - 1001 \right) + 1.03, 2004 \leq x \leq 2010 \end{array} \right.$$

511 From 2002 to 2011, the m-value had a moderately good correlation with the NO_x
512 emission in Ontario (r = 0.91, P<0.01), and the two variables decreased by 30-40% in
513 this period. From 1990 to 2003, the near constant m-value was, however, inconsistent
514 with the bell-shape profile of the NO_x emissions mainly caused by annual variations in
515 NO_x emission from the sector of Transportation and Mobile Equipment in Ontario and
516 Québec, which could be due to either the perturbation from climate anomalies or
517 unrealistic emissions inventory from (APEI) in Canada. Considering that the first
518 possibility was minimal over a large regional scale, especially when the consistency
519 was determined in a different time frame (2002-2011) in the same region, it is thus
520 doubtful that the bell-shape profile of the NO_x emissions in 1990-2003 was realistic.

521

522 The regional m-values of NH_4^+ largely oscillated from 1988 to 2003 (Fig. 5c). The m-
523 values of NH_4^+ , however, decreased by ~30% from 2002 to 2011, leading to a probable
524 decreasing trend in m-value from 1988 to 2011. No correlation was found between the
525 m-values of NH_4^+ and the emissions of NH_3 in Ontario, which is consistent with the
526 findings at the individual sites discussed above.

527

528 Since the decrease in F_{wet} values of NO_3^- at Sites 3 and 4 were very likely due to the
529 mitigation of NO_x in Ontario, the decrease also changed the relative contributions
530 between NH_4^+ and NO_3^- in the total N wet deposition budget. For example, NH_4^+ and
531 NO_3^- contributed 52% and 48%, respectively, to the total budget in 2010-2011 and 34%
532 and 66%, respectively, in 1984-1985 at Site 3. The corresponding numbers at Site 4
533 were 58% and 42% in 2010-2011 and 47% and 53% in 1985-1986.

534

535 **4. Conclusions**

536 Climate anomalies during the two-decade period resulted in annual F_{wet} of SO_4^{2-} and/or
537 NO_3^- deviating from the normal value by up to ~40% at the rural Canadian sites. The
538 new approach of rearranging and screening F_{wet} data can largely reduce the impact of
539 climate anomalies when used for generating the decadal trends of F_{wet} . With the climate
540 perturbation being reduced, F_{wet} of SO_4^{2-} exhibited a three-phase decreasing trend at
541 every individual site, as well as on a regional scale in northern Ontario and Québec.
542 The three-phase pattern of the decreasing trend in F_{wet} of SO_4^{2-} matches well with the
543 emission trends of SO_2 in Ontario, as supported by the good correlation between wet
544 deposition and emission, with $r \geq 0.95$ and $P < 0.01$. F_{wet} of NO_3^- exhibited a two-phase
545 decreasing trend, but only during the second phase F_{wet} of NO_3^- , and the emissions of
546 NO_x in Ontario and Québec matched well, with a good correlation of $r \geq 0.91$ and

547 $P < 0.01$. Compared to the results obtained without applying the new approach, it is
548 concluded that, after reducing the perturbation from climate anomalies, 1) better
549 correlation was obtained between F_{wet} of ions and the emission of the corresponding
550 gaseous precursors in northern Ontario and Québec, and 2) the inflection points in the
551 decreasing trends of F_{wet} of SO_4^{2-} and NO_3^- were visibly and statistically identified.

552

553 However, the new approach cannot completely remove the perturbations from climate
554 anomalies, especially when this is the dominant factor and/or on long timescales, as
555 was the case at a coastal site of Saturna in British Columbia. At this location, the
556 decreasing trends in F_{wet} of SO_4^{2-} and NO_3^- were caused by the decadal anomalies of
557 wind fields, as well as being affected by interannual climate variability including
558 precipitation depth and annual anomalies of wind fields, etc., which overwhelmed the
559 impact of the emission changes of the gaseous precursors in this province. This is the
560 first study that has identified that decadal anomalies of wind fields can dominate trends
561 in F_{wet} of SO_4^{2-} and NO_3^- . The new findings will stimulate more studies on the impacts
562 of decadal climate anomalies on atmospheric deposition of concerned air pollutants.
563 The long-term variations in F_{wet} of NH_4^+ generally showed no clear long-term trends.
564 Moreover, no apparent cause-effect relationships were found between the wet
565 deposition of NH_4^+ and the emission of NH_3 . It can be reasonably inferred that
566 additional key factors besides those discussed in this study also impact the trends of
567 F_{wet} of NH_4^+ . Thus, cautions should be taken to use wet deposition fluxes of NH_4^+ to
568 extrapolate emissions of NH_3 .

569

570 *Data availability.* Data used in this study are available from the corresponding authors.

571 *Supplement.* The supplement materials are available online.

572 *Author contribution.* X. Y. and L. Z. designed the study, analyzed the data and prepared the manuscript.

573 *Competing interests.* The authors declare that they have no conflict of interest.

574 *Acknowledgments.* X.Y. is supported by the National Key Research and Development Program in

575 China (No. 2016YFC0200500), and L.Z. by the Air Pollutants program of Environment and Climate

576 Change Canada.

577

578 **References**

579 Baumgardner, R.E., Lavery, T.F., Rogers, C.M., and Isil, S.S.: Estimates of the Atmospheric
580 Deposition of Sulfur and Nitrogen Species: Clean Air Status and Trends Network,
581 1990–2000, *Environ. Sci. & Technol.*, 36, 2614–2629.
582 <https://doi.org/10.1021/es011146g>, 2002.

583 Bond, N. A., Overland, J. E., Spillane, M., and Stabeno, P.: Recent shifts in the state of the
584 North Pacific, *Geophys. Res. Lett.*, 30, 2183, <https://doi.org/10.1029/2003GL018597>,
585 2003.

586 Burakowski, E. A., Wake, C. P., Braswell, B., and Brown, D. P.: Trends in wintertime climate
587 in the northeastern United States: 1965–2005, *J. Geophys Res. Atmos.*, 113, 1–12.
588 <https://doi.org/10.1029/2008JD009870>, 2008.

589 Butler, T. J., Likens, G. E., Vermeylen, F. M., and Stunder, B. J. B.: The impact of changing
590 nitrogen oxide emissions on wet and dry nitrogen deposition in the northeastern USA,
591 *Atmos. Environ.*, 39, 4851–4862, <https://doi.org/10.1016/j.atmosenv.2005.04.031>, 2005.

592 Cheng, I. and Zhang, L. Long-term air concentrations, wet deposition, and scavenging ratios
593 of inorganic ions, HNO₃, and SO₂ and assessment of aerosol and precipitation acidity at
594 Canadian rural locations, *Atmos. Chem Phys.*, 17, 4711–4730,
595 [https://doi.org/10.5194/acp-17-4711-2017\(2017\)](https://doi.org/10.5194/acp-17-4711-2017(2017)).

596 Coopersmith, E. J., Minsker, B. S., and Sivapalan, M.: Patterns of regional hydroclimatic
597 shifts: An analysis of changing hydrologic regimes, *Water Resour. Res.*, 50, 1960–1983.
598 <https://doi.org/10.1002/2012WR013320>, 2014

599 Deng, Y., Gao, T., Gao, H., Yao, X., and Xie, L.: Regional precipitation variability in East
600 Asia related to climate and environmental factors during 1979–2012, *Scientific Reports*,
601 4, 5693. <https://doi.org/10.1038/srep05693>, 2014.

602 Fagerli, H., and Aas, W.: Trends of nitrogen in air and precipitation: model results and
603 observations at EMEP sites in Europe, 1980–2003, *Environ. Pollut.* 154, 448–461.
604 <https://doi.org/10.1016/j.envpol.2008.01.024>, 2008

605 Fowler, D., Smith, R., Muller, J., Cape, J. N., Sutton, M., Erisman, J. W., and Fagerli, H.:
606 Long Term Trends in Sulphur and Nitrogen Deposition in Europe and the Cause of
607 Non-linearities, *Water Air Soil Pollut.*, 7, 41–47. <https://doi.org/10.1007/s11267-006-9102-x>, 2007.

609 Fowler, D., Smith, R. I., Muller, J. B. A., Hayman, G., and Vincent, K. J.: Changes in the
610 atmospheric deposition of acidifying compounds in the UK between 1986 and 2001,
611 *Environ. Pollut.*, 137, 15–25, <https://doi.org/10.1016/j.envpol.2004.12.028>, 2005.

612 Kampata, J. M., Parida, B. P., and Moalafhi, D. B.: Trend analysis of rainfall in the
613 headstreams of the Zambezi River Basin in Zambia, *Phys. Chem. Earth*, 33, 621–625,
614 <https://doi.org/10.1016/j.pce.2008.06.012>, 2008.

615 Lajtha, K., and Jones, J.: Trends in cation, nitrogen, sulfate and hydrogen ion concentrations
616 in precipitation in the United States and Europe from 1978 to 2010: a new look at an old

- 617 problem, *Biogeochemistry*, 116, 303–334. <https://doi.org/10.1007/s10533-013-9860-2>,
618 2013.
- 619 Lehmann, C. M. B., Bowersox, V. C., Larson, R. S., and Larson, S. M.: Monitoring Long-
620 term Trends in Sulfate and Ammonium in US Precipitation: Results from the National
621 Atmospheric Deposition Program/National Trends Network, *Water Air Soil Pollut.*, 7,
622 59–66. <https://doi.org/10.1007/s11267-006-9100-z>, 2007.
- 623 Li, Y., Schichtel, B. A., Walker, J. T., Schwede, D. B., Chen, X., Lehmann, C. M. B.,
624 Puchalski, M.A., Gay, D.A., and Collett, J. L.: Increasing importance of deposition of
625 reduced nitrogen in the United States, *Proc. Natl. Acad. Sci. U.S.A.*, 113, 5876–5879,
626 <https://doi.org/10.1073/pnas.1525736113>, 2016.
- 627 Lloret, J., and Valiela, I.: Unprecedented decrease in deposition of nitrogen oxides over North
628 America: the relative effects of emission controls and prevailing air-mass trajectories.
629 *Biogeochemistry*, 129, 165–180. <https://doi.org/10.1007/s10533-016-0225-5>, 2016.
- 630 Lynch, J. A., Bowersox, V. C., and Grimm, J. W.: Acid rain reduced in Eastern United States,
631 *Environ. Sci. Technol.*, 34, 940–949. <https://doi.org/10.1021/es9901258>, 2000.
- 632 Marchetto, A., Rogora, M., and Arisci, S.: Trend analysis of atmospheric deposition data: A
633 comparison of statistical approaches, *Atmos. Environ.*, 64, 95–102,
634 <https://doi.org/10.1016/j.atmosenv.2012.08.020>, 2013.
- 635 Mesinger, F., DiMego, G., Kalnay, E., Mitchell, K. and Coauthors, 2006: North American
636 Regional Reanalysis. *Bulletin of the American Meteorological Society*, 87, 343–360,
637 doi:10.1175/BAMS-87-3-343.
- 638 Monteith, D., Henrys, P., Banin, L., Smith, R., Morecroft, M., Scott, T., Andrew, C.
639 Beaumont, D., Benham, S., Bowmaker, V., Corbet, S., Dick, J., Dod, B., Dodd, N.,
640 McKenna, C., McMillan, S., Pallett, D., Pereira, M.G., Poskitt, J., Rennie, S., Rose,
641 R., Schäfer, S., Sherrin, L., Tang, S., Turner, A., and Watson, H.: Trends and
642 variability in weather and atmospheric deposition at UK Environmental Change
643 Network sites (1993–2012), *Ecol. Indic.*, 68, 21–35.
644 <https://doi.org/10.1016/j.ecolind.2016.01.061>, 2016.
- 645 Pihl Karlsson, G., Akselsson, C., Hellsten, S., and Karlsson, P. E.: Reduced European
646 emissions of S and N – Effects on air concentrations, deposition and soil water
647 chemistry in Swedish forests, *Environ. Pollut.*, 159(12), 3571–
648 3582, <https://doi.org/10.1016/j.envpol.2011.08.007>, 2011.
- 649 Rogora, M., Colombo, L., Marchetto, A., Mosello, R., and Steingruber, S.: Temporal and
650 spatial patterns in the chemistry of wet deposition in Southern Alps, *Atmos. Environ.*,
651 146, 44–54. <https://doi.org/10.1016/j.atmosenv.2016.06.025>, 2016.
- 652 Rogora, M., Mosello, R., and Marchetto, A.: Long-term trends in the chemistry of
653 atmospheric deposition in Northwestern Italy: The role of increasing Saharan dust
654 deposition. *Tellus B Chem. Phys. Meteorol.*, 56, 426–434.
655 <https://doi.org/10.1111/j.1600-0889.2004.00114.x>, 2004.
- 656 Ryan, S.E. and Porth, L.S.: A tutorial on the piecewise regression approach applied to
657 bedload transport data, General Technical Report RMRS-GTR-189,
658 https://www.fs.fed.us/rm/pubs/rmrs_gtr189.pdf, 2007.
- 659 Sickles II, J. E., and Shadwick, D. S.: Air quality and atmospheric deposition in the eastern
660 US: 20 years of change, *Atmos. Chem. Phys.*, 15, 173–197. <https://doi.org/10.5194/acp-15-173-2015>, 2015.
- 662 Strock, K. E., Nelson, S. J., Kahl, J. S., Saros, J. E., and McDowell, W. H.: Decadal Trends
663 Reveal Recent Acceleration in the Rate of Recovery from Acidification in the
664 Northeastern U.S., *Environ. Sci. Technol.*, 48, 4681–4689.
665 <https://doi.org/10.1021/es404772n>, 2014.

666 Teng, X., Hu, Q., Zhang, L.M., Qi, J., Shi, J., Xie, H., Gao, H.W., and Yao, X.H.:
667 Identification of major sources of atmospheric NH₃ in an urban environment in northern
668 China during wintertime, *Environ. Sci. Technol.*, 51, 6839–6848, [https://](https://doi.org/10.1021/acs.est.7b00328)
669 10.1021/acs.est.7b00328, 2017.

670 van Donkelaar, A., R. V. Martin, R. Leaitch, A. M. Macdonald, T. W. Walker, D. Streets, Q.
671 Zhang, E. J. Dunlea, J. Jimenez-Palacios, J. Dibb, L. G. Huey, R. Weber, and M. O.
672 Andreae.: Analysis of aircraft and satellite measurements from the Intercontinental
673 Chemical Transport Experiment (INTEX-B) to quantify long-range transport of East
674 Asian sulfur to Canada, *Atmos. Chem. Phys.*, 8, 2999-3014, [https://doi:10.5194/acp-8-](https://doi.org/10.5194/acp-8-2999-2008)
675 2999-2008, 2008.

676 Vet, R., Artz, R. S., Carou, S., Shaw, M., Ro, C.-U., Aas, W., Baker, A., Bowersox, V.C.,
677 Dentener, F., Galy-Lacaux, C., Hou, A., Pienaar, J.J., Gilletti, R., Forti, C., Gromov, S.,
678 Hara, H., Khodzher, T., Mahowald, N.M., Nickovic, S., Rao, P.S.P., and Reid, N. W. A
679 global assessment of precipitation chemistry and deposition of sulfur, nitrogen, sea salt,
680 base cations, organic acids, acidity and pH, and phosphorus, *Atmos. Environ.*, 93, 3–
681 100. <https://doi.org/10.1016/j.atmosenv.2013.10.060>, 2014.

682 Vet, R., and Ro, C.-U.: Contribution of Canada–United States transboundary transport to wet
683 deposition of sulphur and nitrogen oxides—A mass balance approach, *Atmos. Environ.*,
684 42, 2518–2529. <https://doi.org/10.1016/j.atmosenv.2007.12.034>, 2008.

685 Waldner, P., Marchetto, A., Thimonier, A., Schmitt, M., Rogora, M., Granke, O., Mues, V.,
686 Hansen, K., Pihl Karlsson, G., Zlindra, D., Clarke, N., Verstraeten, A., Lazdins, A.,
687 Schimming, C., Iacoban, C., Lindroos, A.-J, Vanguelova, E., Benham, S., Meesenburg,
688 H., Nicolau, M., Kowalska, A., Apuhtin, V., Napa, U., Lachmanova, Z., Kristoefel, F.,
689 Bleeker, A., Ingerslev, M., Vesterdal, L., Molina, J., Fischer, U., Seidling, W., Jonard,
690 M., O’Dea, P., Johnson, J., Fischer, R., and Lorenz, M.: Detection of temporal trends in
691 atmospheric deposition of inorganic nitrogen and sulphate to forests in Europe, *Atmos.*
692 *Environ.*, 95, 363-37. <http://dx.doi.org/10.1016/j.atmosenv.2014.06.054>, 2014.

693 Wetherbee, G. A., and Mast, M. A.: Annual variations in wet-deposition chemistry related to
694 changes in climate, *Clim. Dynam.*, 47, 3141–3155, [https://doi.org/10.1007/s00382-016-](https://doi.org/10.1007/s00382-016-3017-7)
695 3017-7, 2016.

696 Wijngaard, J. B., Tank, A. M. G. K., and Können, G. P.: Homogeneity of 20th century
697 European daily temperature and precipitation series. *Int. J. Climatol.*, 23, 679–692,
698 <https://doi.org/10.1002/joc.906>, 2003.

699 Wright L.P., Zhang L., Cheng I., Aherne J., and Wentworth G.R.: Impacts and effects
700 indicators of atmospheric deposition of major pollutants to various ecosystems – A
701 review. *Aerosol Air Qual. Res.*, 18, 1953-1992, doi: 10.4209/aaqr.2018.03.0107, 2018

702 Wu, Z., and Huang, N. E.: Ensemble empirical mode decomposition: a noise-assisted data
703 analysis method. *Advances in Adaptive Data Analysis*, 1, 1–41,
704 <https://doi.org/10.1142/S1793536909000047>, 2009

705 Vieth, E.: Fitting piecewise linear regression functions to biological responses, *J. Appl.*
706 *Physiol.*, 67, 390–396, doi:10.1152/jappl.1989.67.1.390, 1989.

707 Yao, X. H., and Zhang, L. Supermicron modes of ammonium ions related to fog in rural
708 atmosphere, *Atmos. Chem. Phys.*, 12, 11165–11178, [https://doi.org/10.5194/acp-12-](https://doi.org/10.5194/acp-12-11165-2012)
709 11165-2012, 2012

710 Yao, X., and Zhang, L. Trends in atmospheric ammonia at urban, rural, and remote sites
711 across North America, *Atmos. Chem. Phys.*, 16, 11465–11475,
712 <https://doi.org/10.5194/acp-16-11465-2016>, 2016.

713 Zbieranowski, A.L. and Aherne, J.: Long-term trends in atmospheric reactive nitrogen across
714 Canada: 1988–2007, *Atmos. Environ.*, 45, 5853-5862,

- 715 <https://doi.org/10.1016/j.atmosenv.2011.06.080>, 2011.
- 716 Zhang, L., Jacob, D. J., Knipping, E. M., Kumar, N., Munger, J. W., Carouge, C. C., van
717 Donkelaar, A., Wang, Y.X., and Chen, D.: Nitrogen deposition to the United States:
718 Distribution, sources, and processes, *Atmos. Chem. Phys.*, 12, 4539–4554,
719 <https://doi.org/10.5194/acp-12-4539-2012>, 2012.
- 720 Zhang, L., Vet, R., Wiebe, A., and Mihele, C.: Characterization of the size-segregated water-
721 soluble inorganic ions at eight Canadian rural sites, *Atmos. Chem. Phys.*, 8, 7133–7151,
722 <https://doi.org/10.5194/acp-8-7133-2008>, 2008.

List of Figures

Figure 1. Fitting monthly F_{wet} of SO_4^{2-} against the climatology values from every two years using LR with zero interception at Site 1 according to the new approach described in Section 2. Fitted lines represent the LR function with zero interception using 24 elements. x , y and R^2 in the legend represent climatology monthly F_{wet} , monthly F_{wet} in every two-year and the coefficient of determination in LR analysis, respectively. * reflects the maximum value (cycled markers) excluded for LR analysis and all P values <0.01 .

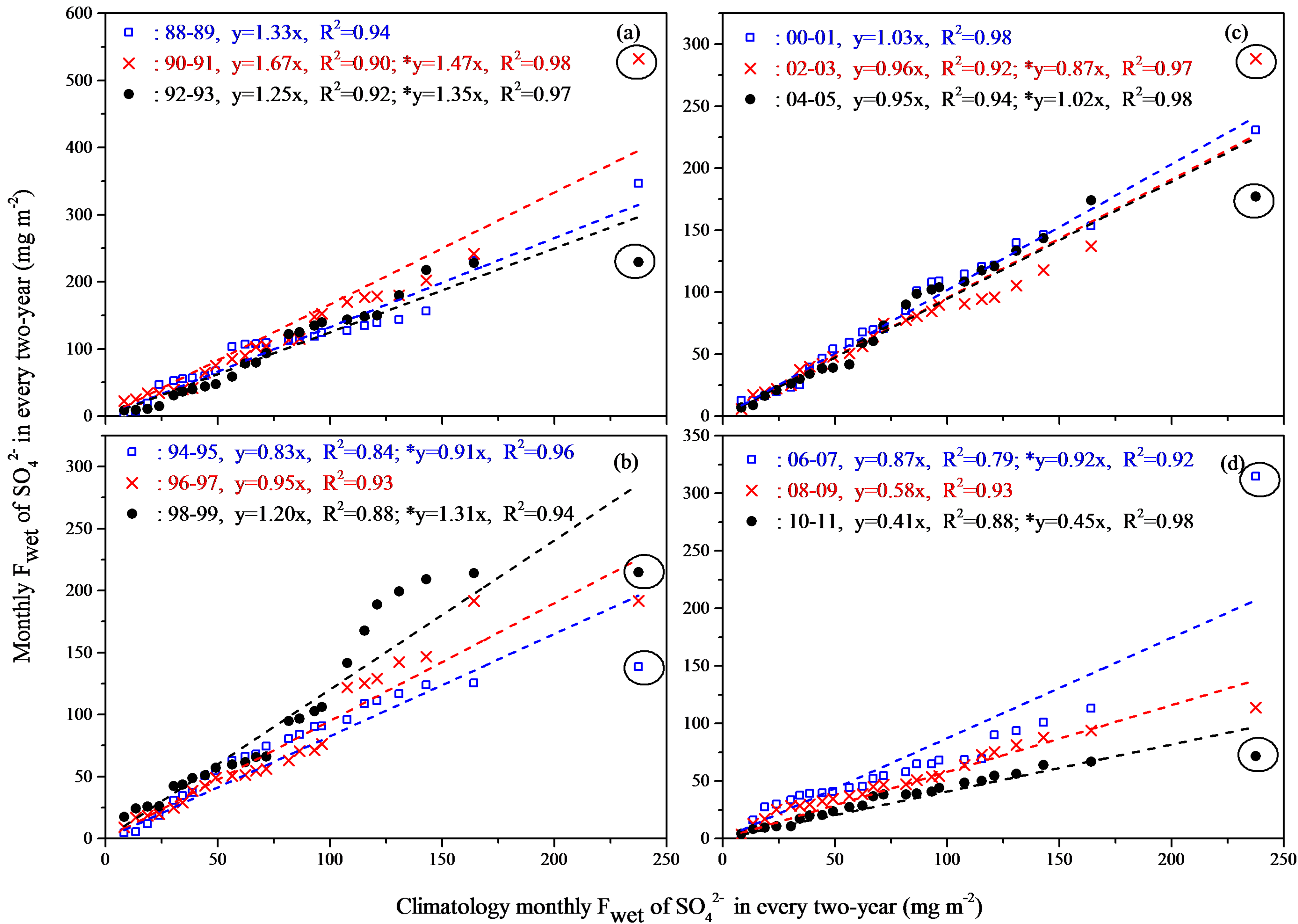
Figure 2. m-values and annual F_{wet} of SO_4^{2-} , NO_3^- and NH_4^+ in 1988-2011 at Site 1, and the annual emissions of SO_2 and NO_x in 1990-2011 in Québec and Ontario, Canada. Full and empty markers in blue in (a), (d) and (g) represent the calculation of m-values without and with the outlier, respectively. Empty markers in red represent the outliers in m-values and are excluded for trend analysis, as detailed in Section 2. R^2 reflects the coefficient of determination of a variable against the calendar year from LR analysis, and the fitted lines represent the LR function. M-K results are shown in (a-b), (d-e) and (g-h). Phases 1, 2 and 3 in (a) and (c), Phases 1 and 2 in (d) and (f) were gained from PLR presented in Section 3.1.

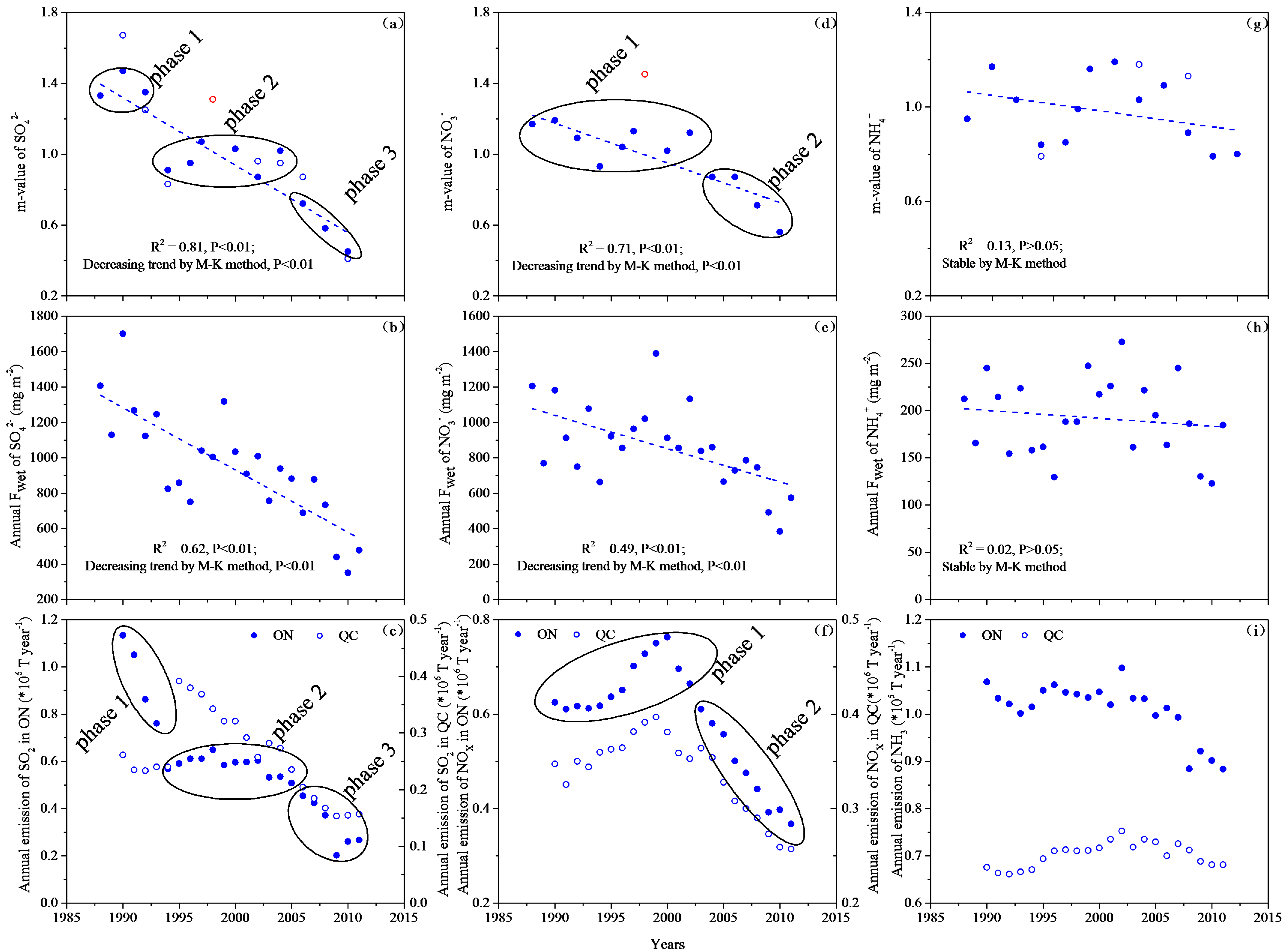
Figure 3. Same as in Fig. 2 except for Site 2, and the annual precipitation and annual emissions in British Columbia, Canada. Horizontal dashes in (b) represent precipitation, and the fitted lines represent the LR function.

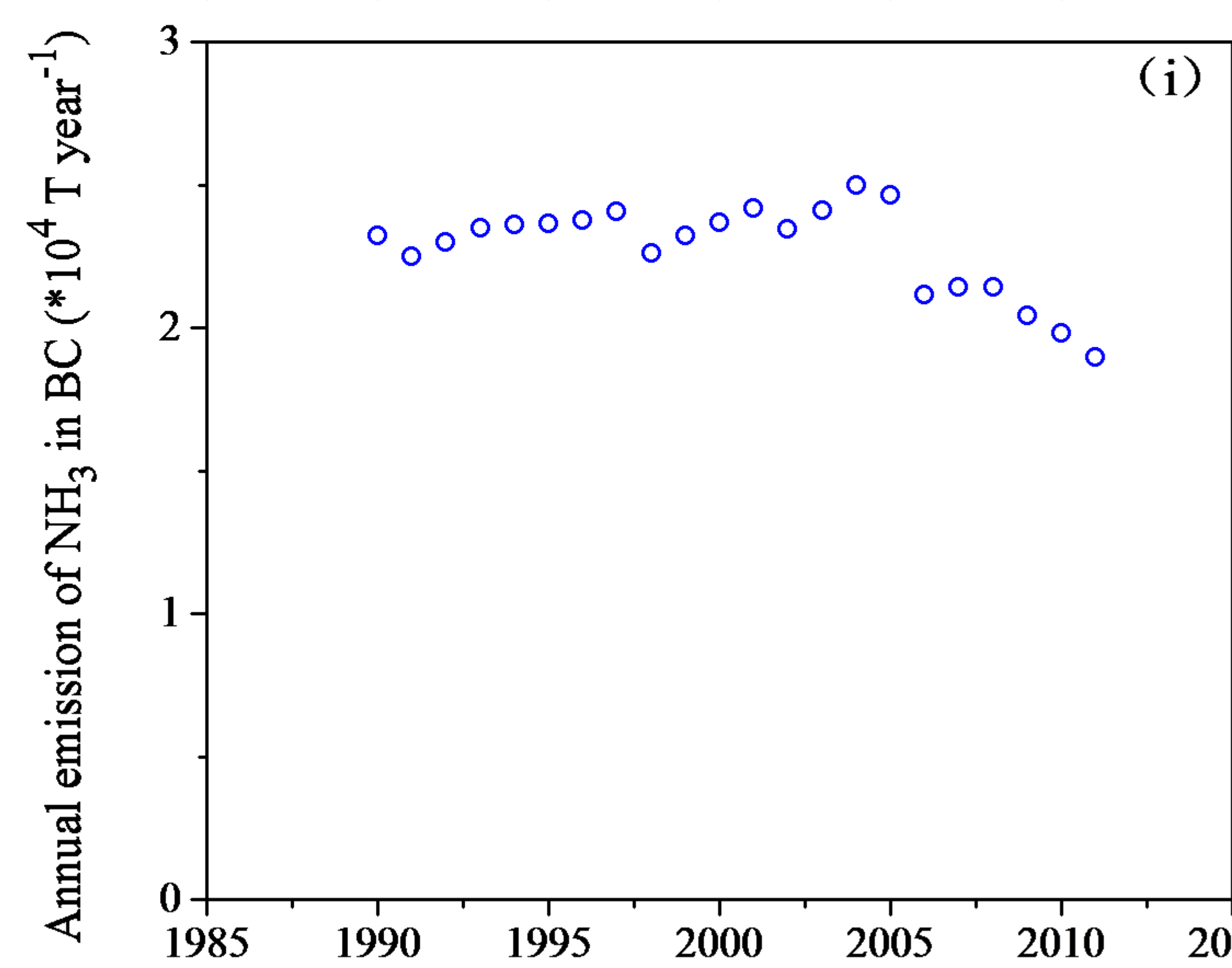
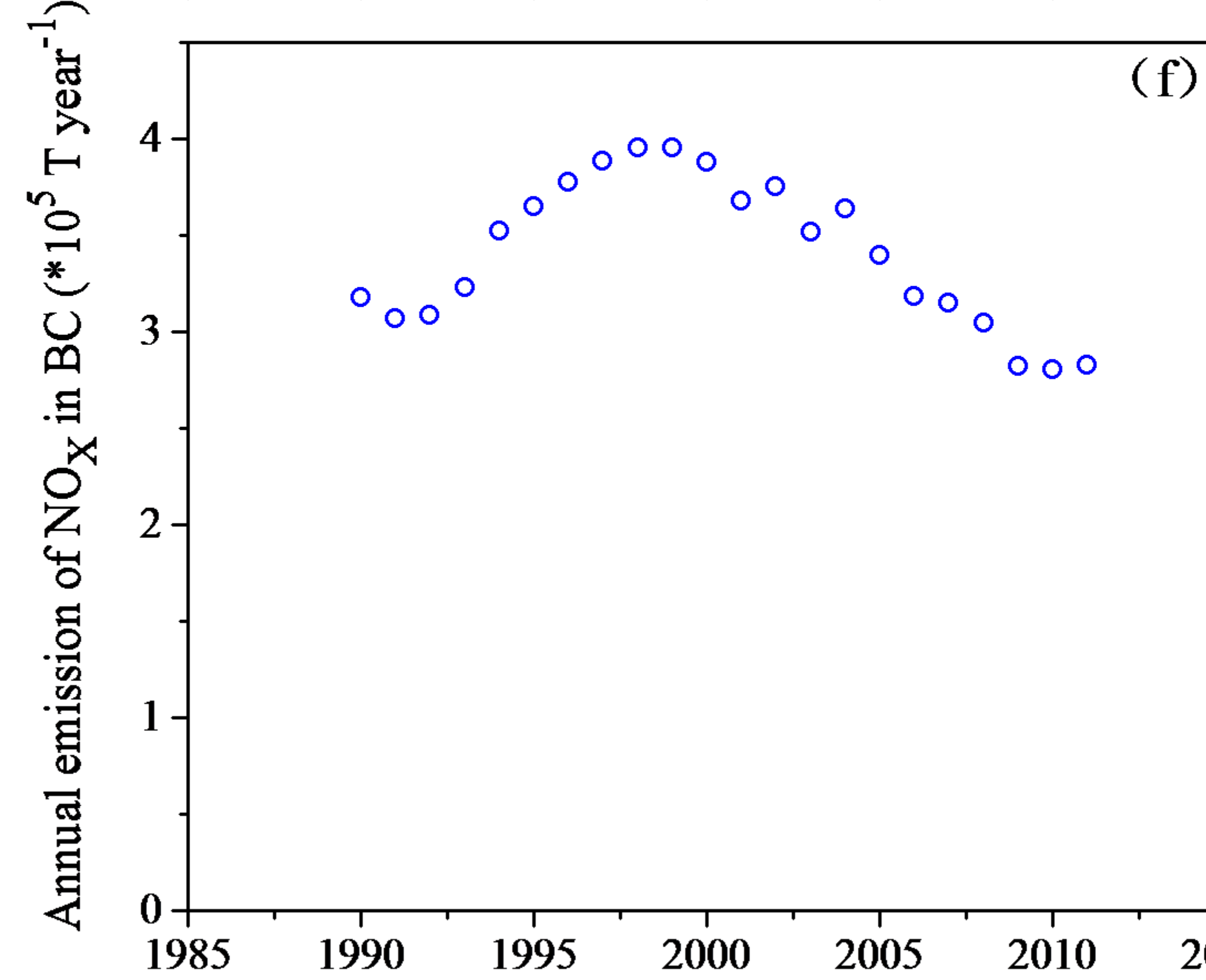
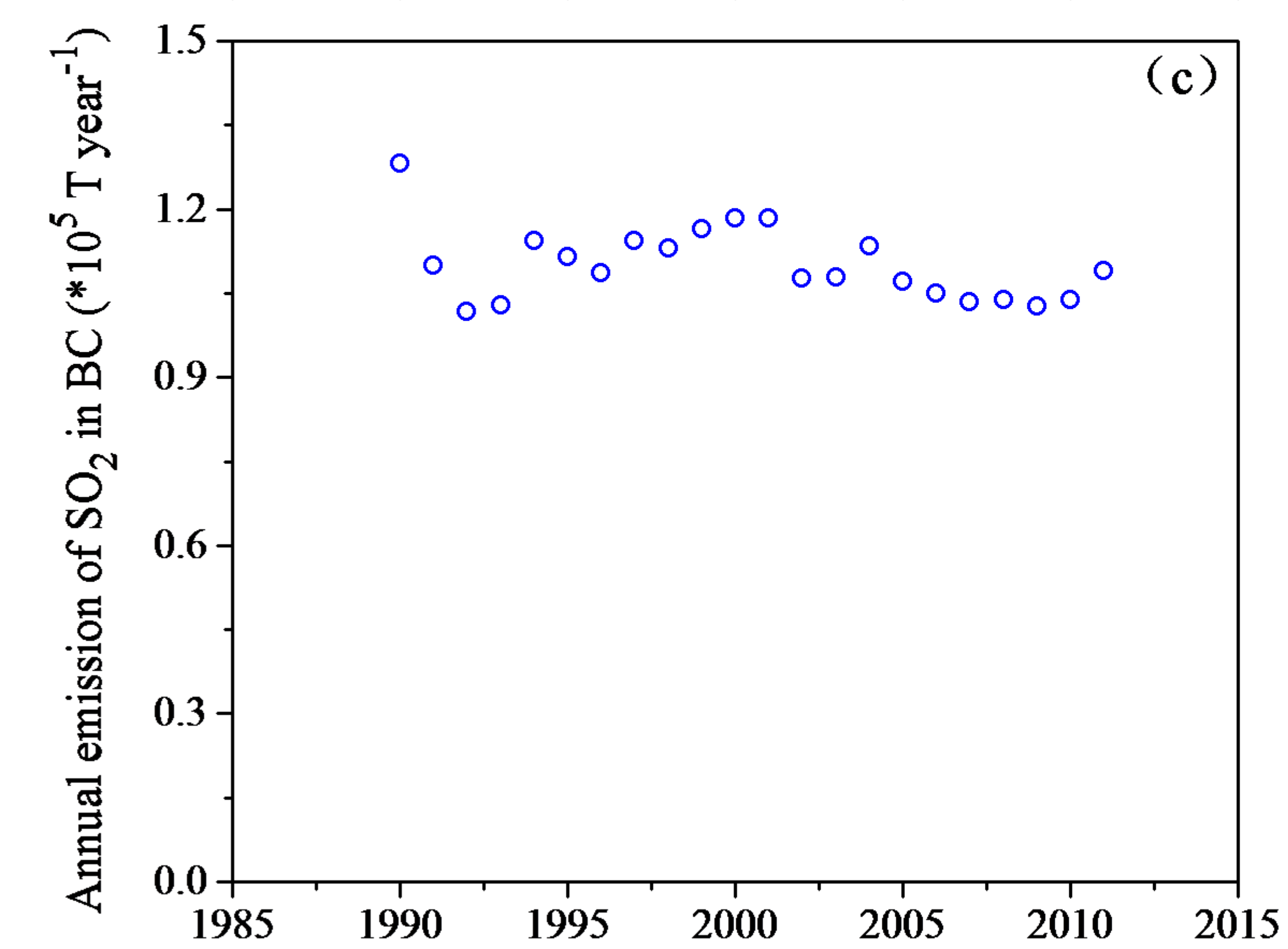
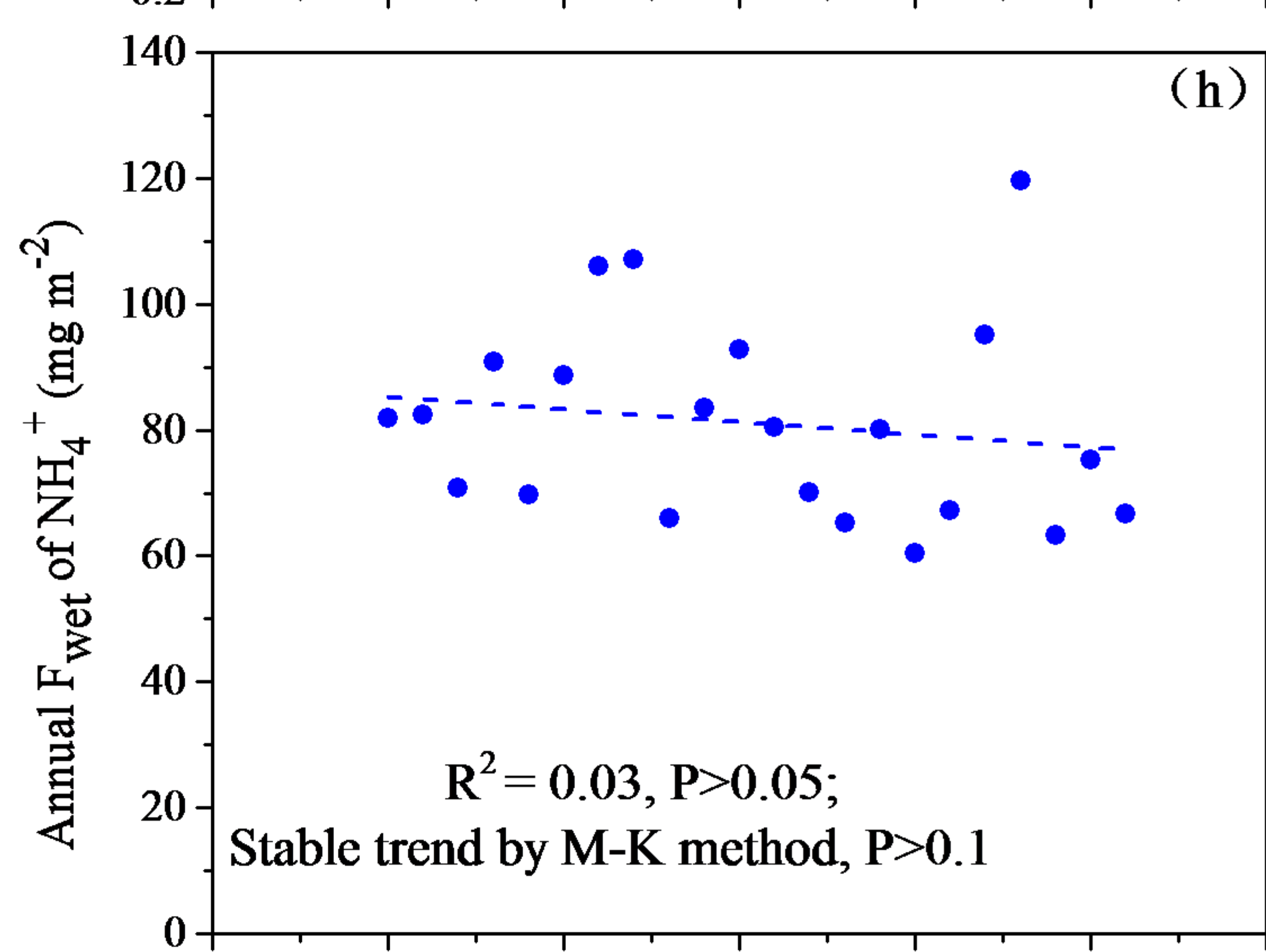
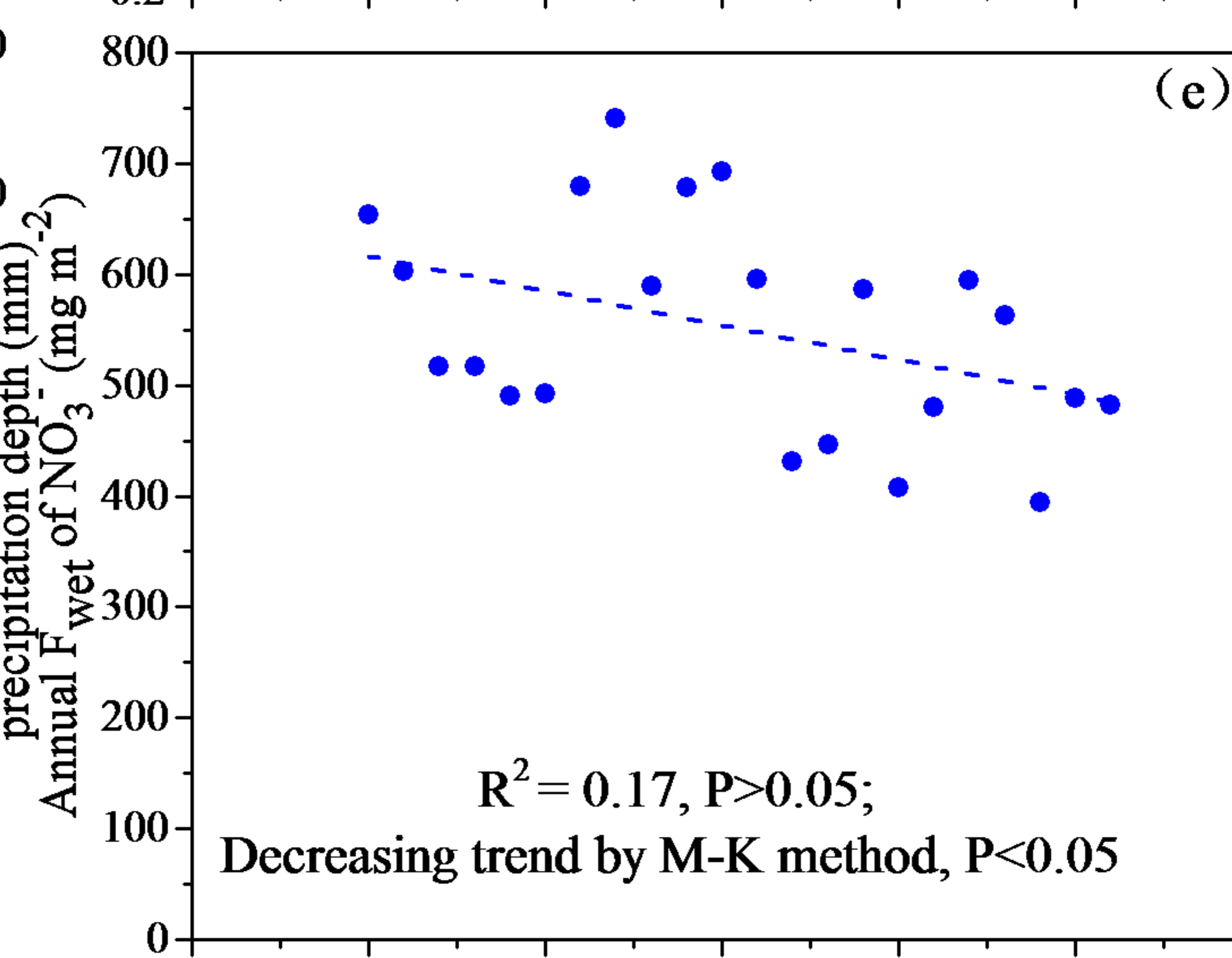
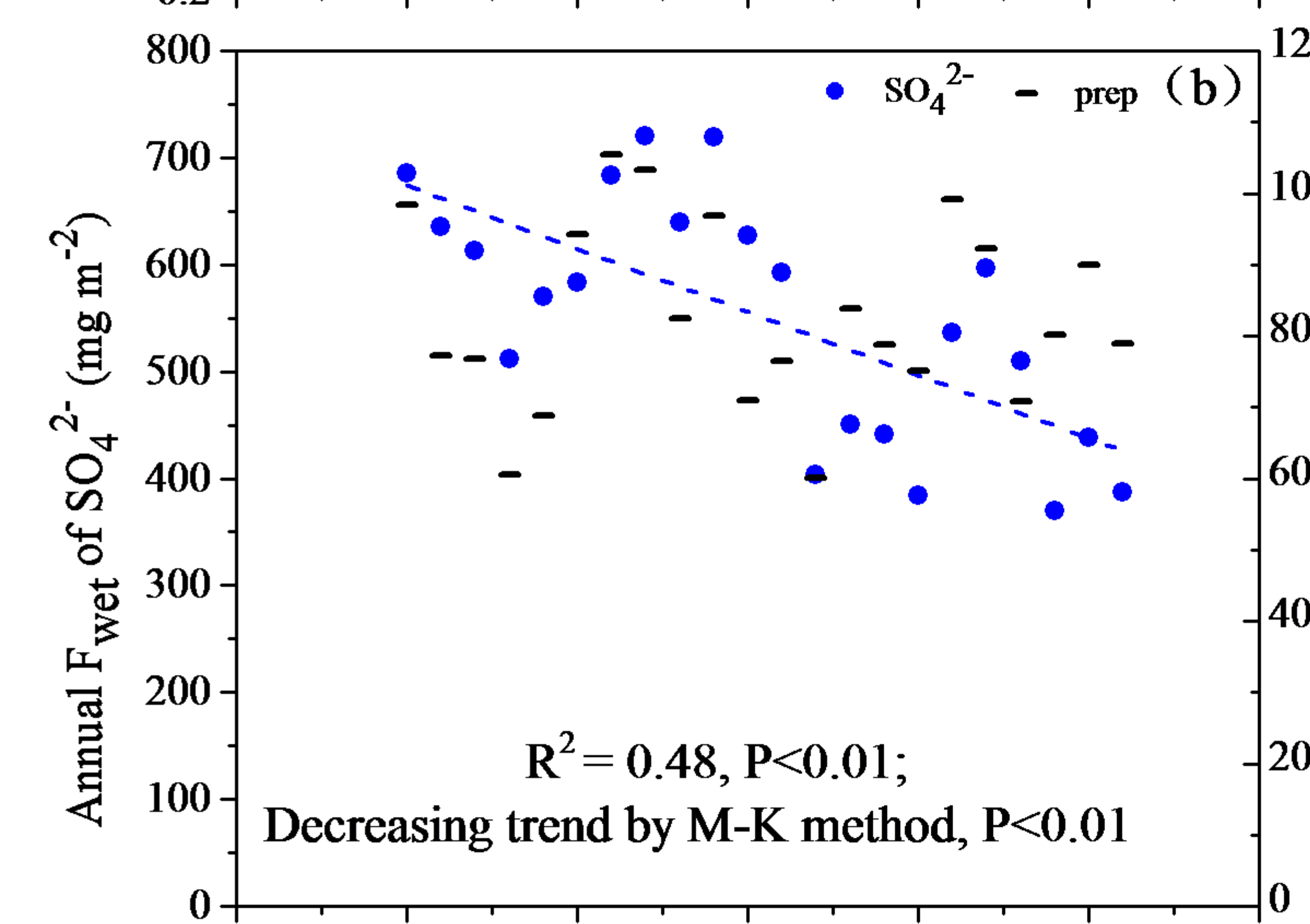
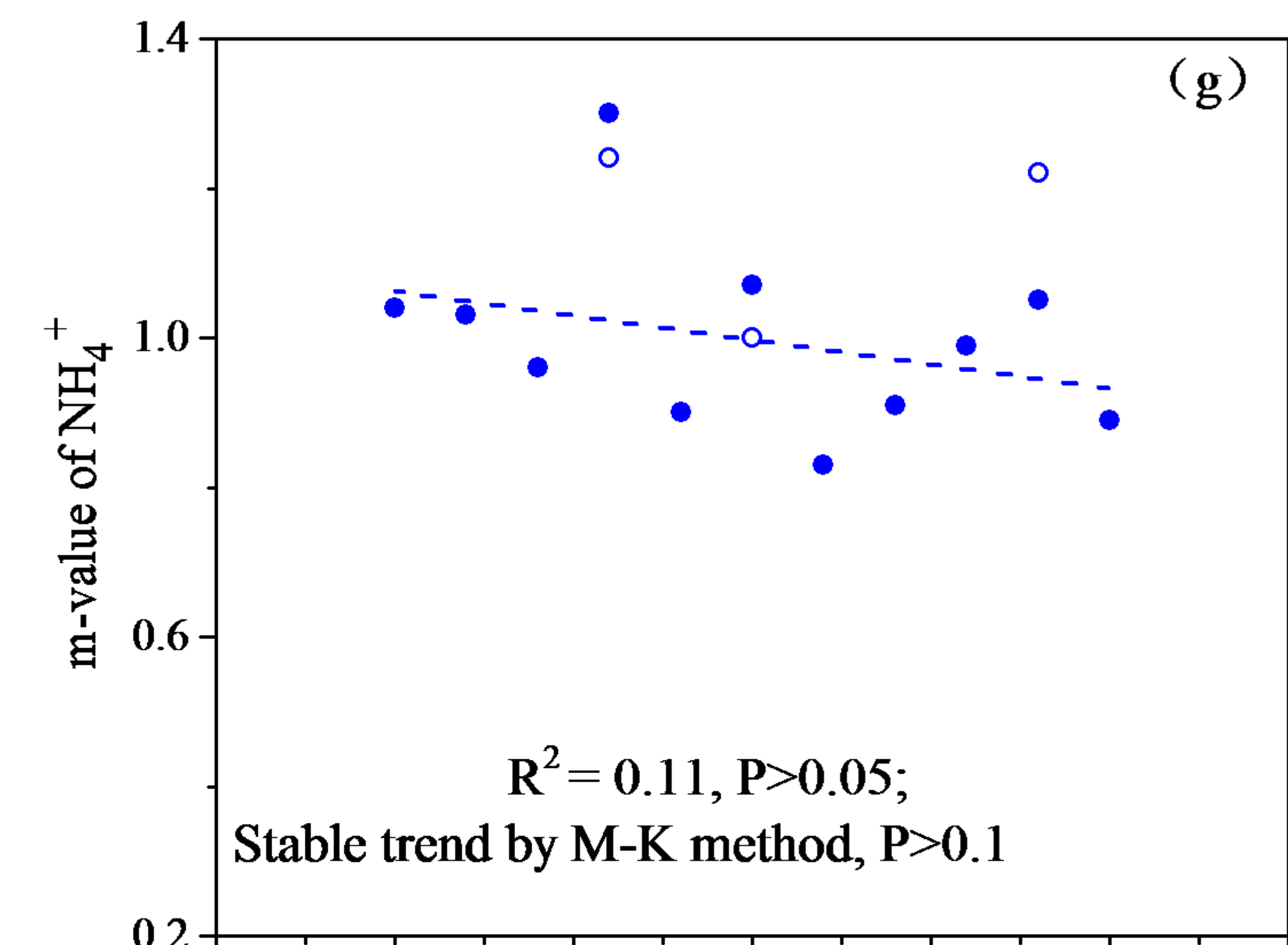
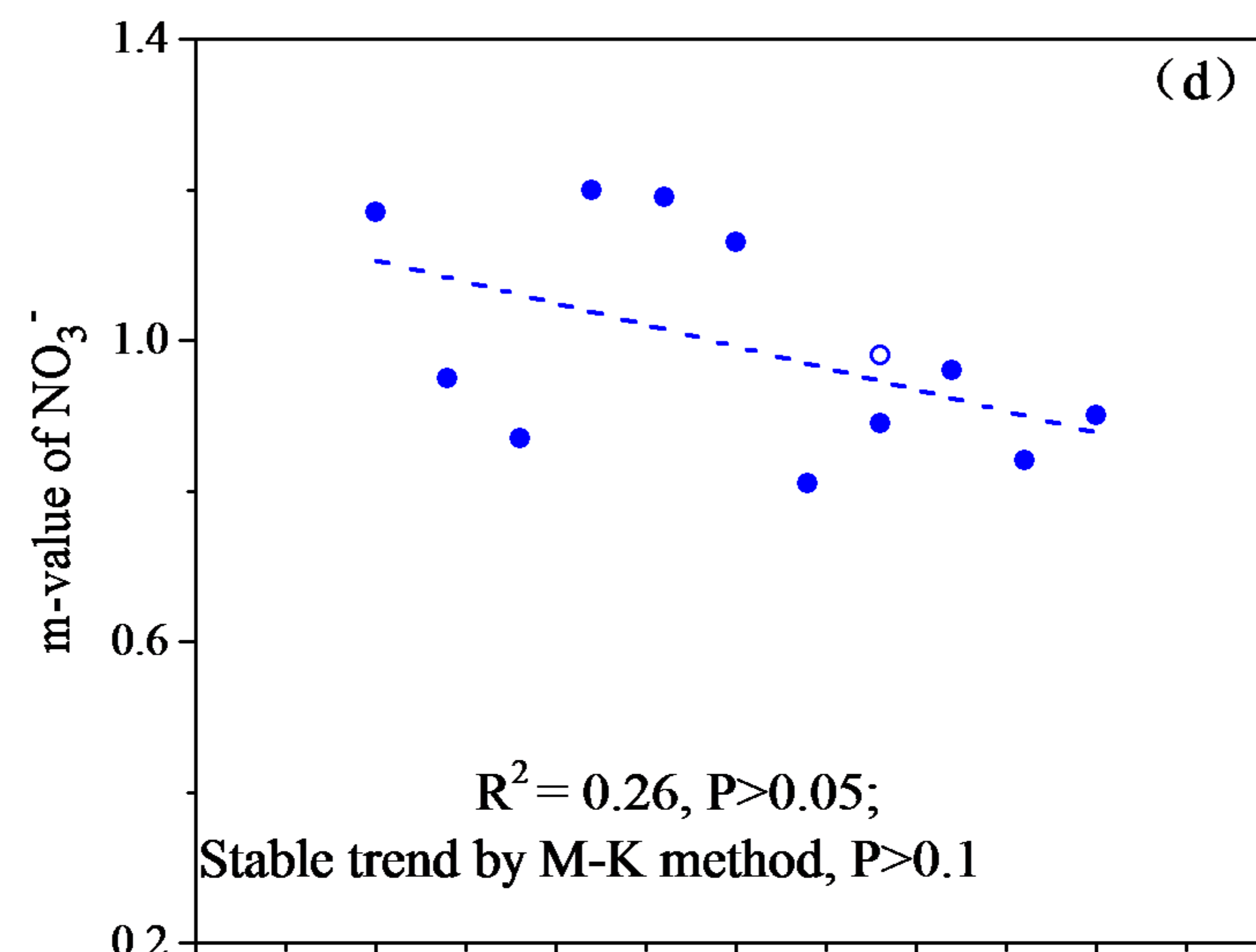
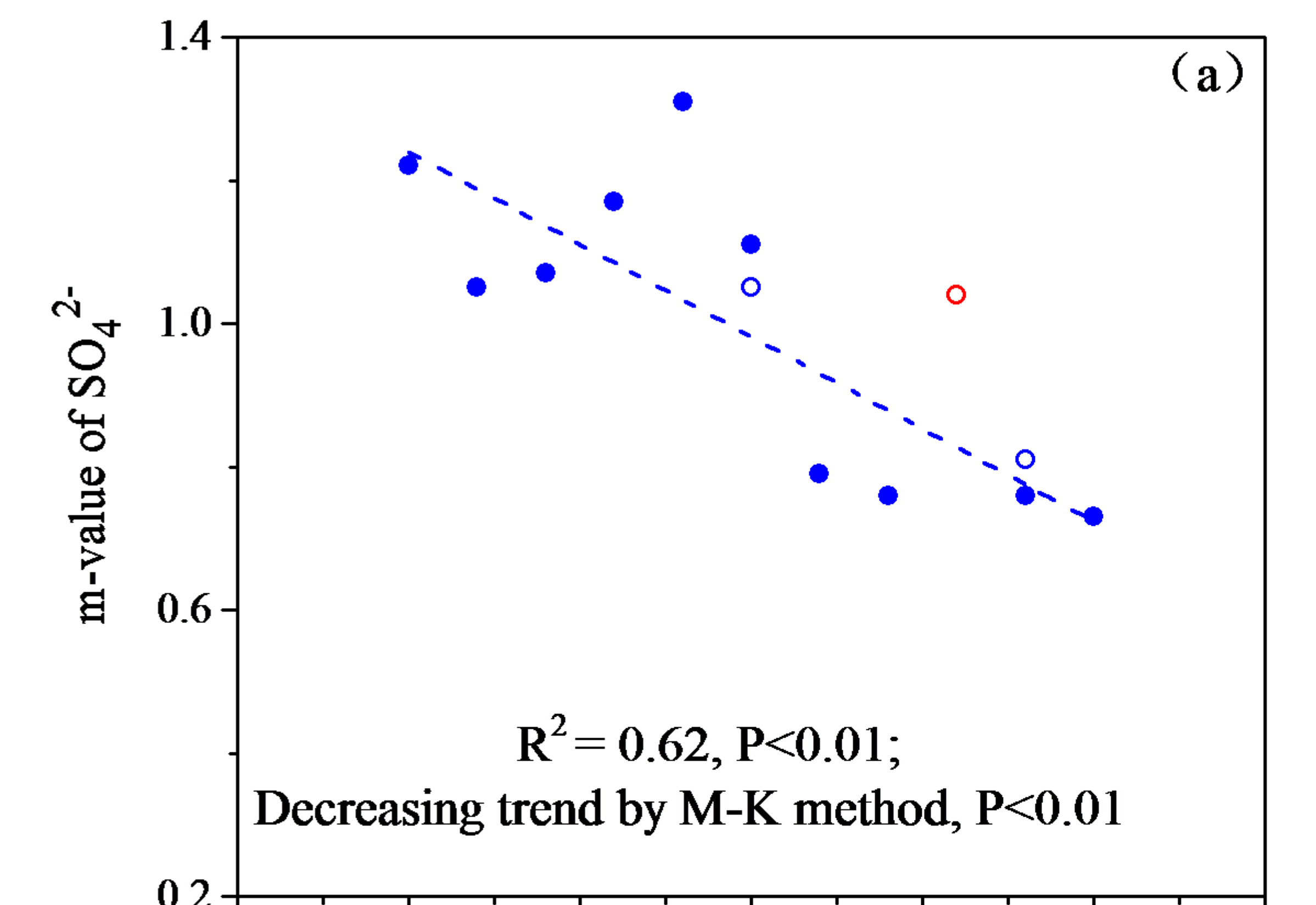
Figure 4. The mean wind vector and speed (shading area) during 1990-2011 (a), the anomalies of wind vector and wind speed (shading area) during 1990-2001 (b), 2002-2011 (c) and 2007 (d) at 925 hPa over the western coastal Canada and U.S. (the anomalies in b, c and d were conducted relative to the 20-year period of 1990-2009 and the wind vector and wind speed were from the North American Regional Reanalysis (NARR) with a spatial resolution of 32 km by 32 km).

Figure 5. Regional m-values at Sites 1, 3 and 4: (a): SO_4^{2-} , (b): NO_3^- , and (c): NH_4^+ . R^2 reflects the coefficient of determination of a variable against the calendar year from LR analysis, and the fitted lines represent the LR function. M-K

results are shown in (a-c). Phases 1, 2 and 3 are shown in (a) and (c). Phases 1 and 2 in (a) and (b) were gained from PLR presented in Section 3.3.

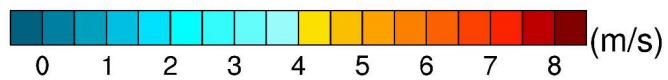
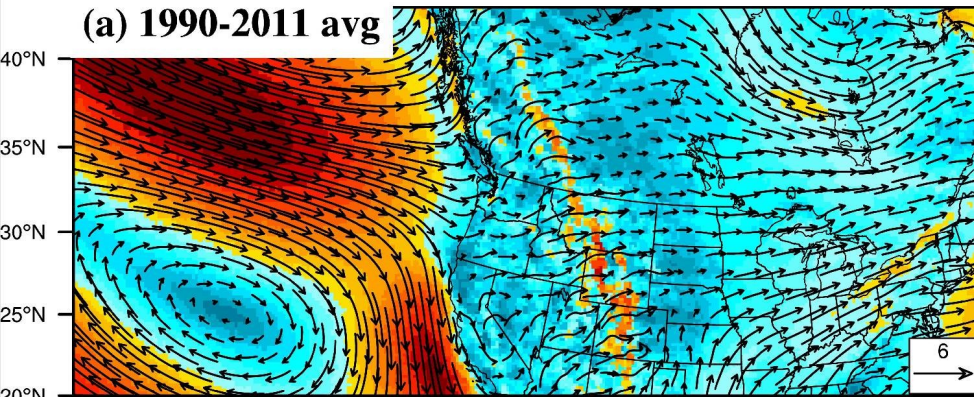




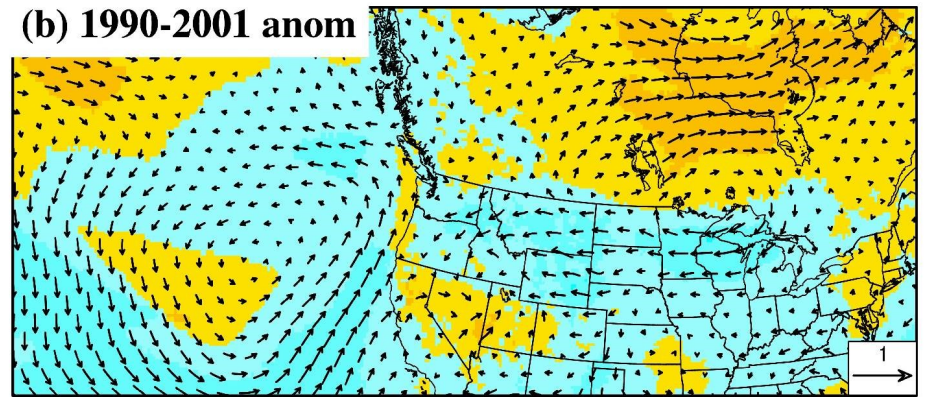


Years

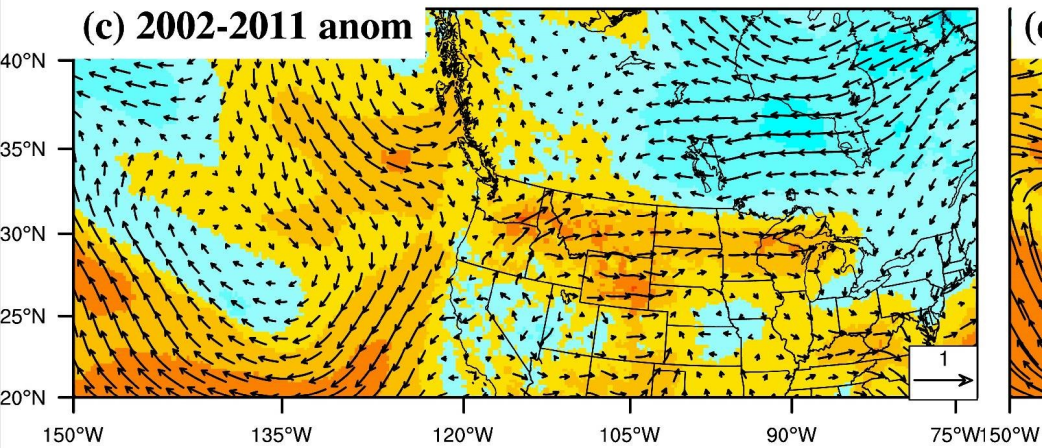
(a) 1990-2011 avg



(b) 1990-2001 anom



(c) 2002-2011 anom



(d) 2007 anom

